Water Coning In Permeable Faults

A thesis submitted to the
Chair of Reservoir Engineering
in partial fulfilment of the requirements for the
Degree of Master of Science

by

Jan Galijasevic

Montan Universität Leoben
Styria, Austria
February 2015

Abstract

The main objective of this thesis is to provide insight into the water coning behavior of wells drilled into permeable geological faults in clastic as well as in naturally fractured basement reservoirs. In both cases a vertical fault with large lateral and vertical extent is considered as a flow zone for oil and water and is produced by a horizontal well placed at the center of the domain. If a certain maximum water-free production rate is exceeded, an early inflow of water into the well can be expected, referred to as water coning. This thesis provides an analytical solution for this maximum water-free production rate which is afterwards used to verify 2D simulations in clastic and naturally fractured reservoirs. All the simulations are run with the commercial CFD software ANSYS Fluent. Additionally, the influence of inertia, boundary effects and different fault parameters on the pressure drop is discussed. The analytical solution for the maximum water-free production rate in case of laminar flow in a fault with specified permeability, as expected in sandstone reservoirs, results in a value of $2.59 \cdot 10^{-6}$ m^3/s. In comparison, the numerical solution yields a higher value of $1.13 \cdot 10^{-5}$ m^3/s resulting in a relative error of 0.8. Using the assumption of a permeability based on the parallel-plate model and Forchheimer dominated flow for an idealized case of a conduit in a naturally fractured reservoir, a maximum water-free production rate of $5.36 \cdot 10^{-4}$ m^3/s is determined analytically. By changing the production rate in different simulation scenarios, the numerical solution indicates a rate of $8.48 \cdot 10^{-5}$ m^3/s. In this scenario turbulent flow behavior is monitored and a relative error of 3.3 observed.

Kurzfassung

Das Hauptziel dieser Abschlussarbeit ist es, einen Einblick in das Verhalten der Wasserkegelbildung durch Bohrungen in durchlässigen geologischen Störungen in Öllagerstätten, bestehend aus Sandstein als auch aus Kluftgestein, zu geben. In beiden Fällen ist eine vertikale Störung mit großer horizontaler und vertikaler Ausdehnung als Strömungszone für Öl und Wasser in Betracht gezogen worden und wird durch eine zentrale Horizontalbohrung produziert. Wenn eine bestimmte maximale wasserfreie Produktionsrate überschritten wird, kann ein verfrühtes Einströmen von Wasser in die Bohrung erfolgen, welches als Wasserkegelbildung bezeichnet wird. Diese Arbeit stellt eine analytische Lösung für diese maximale wasserfreie Produktionsrate dar, die später verwendet wurde, um zweidimensionale Simulationen für klastische und natürlich geklüftete Lagerstätten zu bekräftigen. Alle Simulationen werden mit der kommerziellen CFD-Software ANSYS Fluent durchgeführt. Zusätzlich werden Auswirkungen auf den Druckabfall durch Trägheit, Randbedingungen und variierende Parameter der Störung untersucht. Die analytische Lösung für die maximale wasserfreie Produktionsrate im Fall einer laminaren Strömung in einer Störung mit festgelegter Permeabilität ergibt einen Wert von $2{,}59 \cdot 10^{-6}$ m^3/s. Im Vergleich dazu, resultiert die numerische Lösung in einem höheren Wert von etwa $1{,}13 \cdot 10^{-5}$ m^3/s, welches einen relativen Fehler von 0,8 zur Folge hat. Unter der Annahme einer Permeabilität auf der Basis eines Models bestehend aus zwei parallelen Platten und Forchheimer dominierenden Fließverhalten in den Spalten des Kluftgesteines, wird eine maximale wasserfreie Produktionsrate von $5{,}36 \cdot 10^{-4}$ m^3/s analytisch bestimmt. Eine Veränderung der Eingabe für die Produktionsrate in verschiedenen Simulationsszenarien resultiert in einer numerischen Lösung für eine Produktionsrate von $8{,}48 \cdot 10^{-5}$ m^3/s. In diesem Szenario wird turbulentes Strömungsverhalten und ein relativer Fehler von 3,3 beobachtet.

Eidesstattliche Erklärung

Ich erkläre an Eides statt, dass ich diese Arbeit selbstständig verfasst, andere als die angegebenen Quellen und Hilfsmittel nicht benutzt und mich auch sonst keiner unerlaubten Hilfsmittel bedient habe.

Affidavit

I declare in lieu of oath, that I wrote this thesis and performed the associated research myself, using only literature cited in this volume.

25.02.2015

Unterschrift

Acknowledgements

I wish to express my deepest appreciation to the faculty and staff of the Department of Reservoir Engineering that made great contributions to this work.

First, I would like to thank especially Dr. Matthäi, Chair of Reservoir Engineering at the Montanuniversität of Leoben, for his supervision, encouragement and patience during the completion of this study. Without his faith in me, this thesis would not have been possible.

I also want to thank Caroline Milliotte for her vigorous assistance and support during the building and meshing procedure of the models. She is always able to explain and teach even complex topics in such a motivating and positive way.

Special thanks to PhD candidate Roman Manasipov, a brilliant mathematician who also became a good friend of mine during the development of my work. He was always open to questions of any kind and tried to provide me the best possible advice on how to tackle various difficulties of my thesis.

Last but not least, I like to extend my sincere thanks to Dr. Julian Mindel, Assistant Professor at the Montanuniversität of Leoben, who was my mentor and reference person during the completion of my thesis. Without his distinguished guidance, professional knowledge and generous amount of time I would never be able to finish my study.

Dedication

I would like to dedicate this thesis to my parents for all their love and support needed to complete my study.

Table of Content

List of Figures

List of Tables

Nomenclature

A_c	Flow Cross-Sectional Area, m^2
b	Fracture Aperture, m
B_o	Formation Volume Factor, m^3/sm^3
g	Gravitational Constant, 9.81 m/s^2
h	Oil Column Height, m
h_p	Perforation Interval, m
k	Formation permeability, m^2
k_f	Fracture Permeability, m^2
k_h	Horizontal Permeability, m^2
k_v	Vertical Permeability, m^2
p	Pressure, Pa
q	Fluid Velocity, m/s
Q	Volume Flow Rate, m^3
r	Radius, m
r_c	Critical Radius, m
r_e	Drainage Radius, m
R_e	Reynold's number, -
r_w	Wellbore Radius, m
t	Time, s
u	Fluid velocity, m/s
w	Fracture Width, m
z_c	Critical Vertical Distance, m
α	Volume Fraction, -
β	Forchheimer Correction Term, m^{-1}
θ	Inclination Angle, °
μ_o	Oil Viscosity, Pa s
μ_w	Water Viscosity, Pa s
ρ_o	Oil Density, kg/m^3
ρ_w	Water Density, kg/m^3
ϕ	Porosity, -

Chapter 1

Introduction

Water coning is a common problem in the oil and gas industry and describes basically the upward entrainment of water into the oil zone during production (c.f., Muskat and Wyckoff, 1935; Wheatley, 1985), see Figure 1. This phenomenon occurs when the production rate exceeds a certain critical limit, resulting in a large pressure drawdown around the wellbore. (c.f., Chierici and Ciucci, 1964; Schols, 1972). In this case, dynamic, viscous forces dominate over the gravitational forces between the well and the oil-water contact. The initial flat oil-water contact deforms into a cone, in case of vertical wells, or a crest, for horizontal wells.

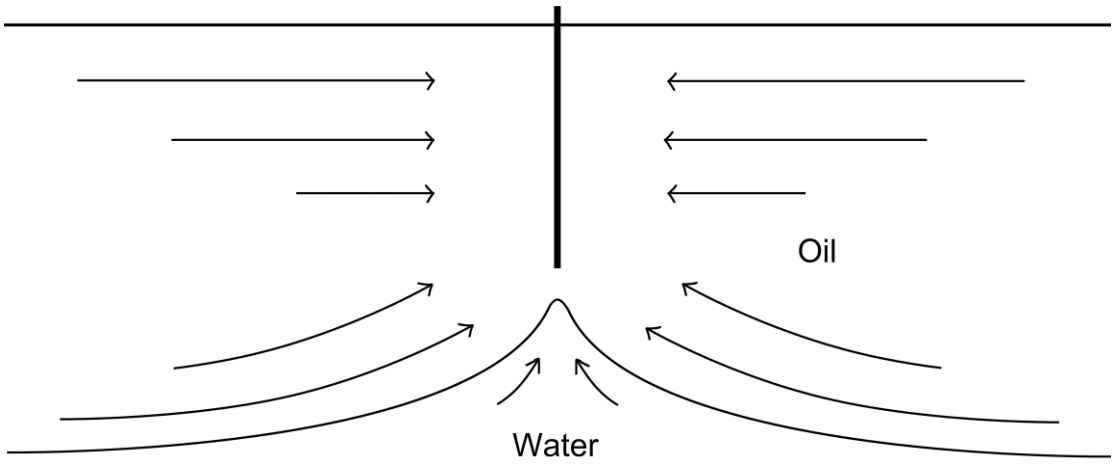

Figure 1 - Illustration of water coning in a vertical well

The development of the cone depends on different variables (c.f., Guo and Lee, 1992; Van Golf-Racht, 1994). One of the most important ones is the distance from the oil-water contact to the well perforations and the density difference between oil and water phase. Additionally, the fluid viscosities, relative permeabilities and the anisotropy of the reservoir also affect the coning behavior.

It is crucial to determine the maximum pressure drawdown around the wellbore to eliminate the problems of coning (Sobocinski, 1965), like increased water cut and therefore additional operational costs which could make operations, e.g. those offshore, uneconomical.

The most common method to lower the pressure gradient and therefore to minimize the risk of early water breakthrough is to reduce the production rate (Chaney et al., 1956). Another possibility is to shut in the well for short period of time to allow the contacts to stabilize again.

Høyland (1989) found that “At a certain production rate, the water cone is stable with its apex at a distance below the bottom of the well, but an infinitesimal rate increase will cause cone instability and water breakthrough. This limiting rate is called the critical rate for water coning.” This critical rate is in most cases notably lower than the potential production rate. Therefore, it has to be evaluated if a reduced production rate is economical feasible or if the risk of water coning should be taken.

It is also often suggested to drill producer wells horizontally since vertical wells with short completion intervals require a larger pressure drawdown to maintain the same oil production rate as horizontal ones (c.f. Chaperon, 1986) and accordingly, the critical rate will be lower than for horizontal wells. For this reason, the production of thin oil columns is possible only with horizontal well technology.

Another strategy is to partially perforate the well in the pay zone or use sliding sleeves to increase the distance from the fluid contacts. However, this solution also decreases the possible oil production rate significantly and that a combination of reduced perforation length and lower production rate is in most cases the best solution (c.f., Chappelear and Hirasaki, 1976).

Since the water coning gives rise to various kinds of problems, many more authors investigated thoroughly the coning development mostly for homogenous, porous formations, by providing methods to determine the critical production rate (steady-state solutions), water breakthrough time and the production performance after (transient solutions).

In this thesis, I will address the water coning behaviour in permeable, geological faults by showing a comparison between different methods to estimate the critical production rate. The literature review covers coning problems in various reservoirs with either vertical or horizontal wells. The obtained knowledge is used to develop an analytical solution for the critical rate of vertical faults with specific porosity and for open fault/fracture conduits in basement rocks. Secondly, CFD simulations are used to analyse this fluid problem, taking into account inertia effects.

The research on this topic is important, because early water breakthrough is a major problem during the production of oil and gas. Therefore, the determination of the maximum free-water production rates in conductive faults is considered to be a major contribution to the awareness of water coning.

This thesis proceeds with an extensive literature review of analytical and numerical studies done on water coning. The development of different approaches and improvements through time are shown in chronological order and give insight into the complexity of the problem. Also a section of inertial effects on flow is provided due to the importance of the topic in naturally fractured reservoirs.

A methodology section follows, describing an approximate analytical solution for the critical rate in conductive, vertical faults with specified, constant permeability has been derived. However, the main focus lies on the case of a thin and open conduit (tank model) with a permeability based on parallel-plate flow. The relevant assumptions, various parameters and the governing equations that depict the coning behavior are presented in a clear way to make the reader understand their influence on early water breakthrough. These analytical solutions have been used to verify the numerical simulations.

The methodology section is followed by the results section. The outcome of the aforedescribed analytical determination of the critical rate and of different simulation runs are presented and explained. Various illustrations are included to communicate the development of the water cone.

A discussion of the obtained results follows and after the conclusion, I will address possible areas for future research.

Chapter 2

Literature Review

2.1 Literature Review on Water Coning

In 1935, Muskat and Wyckoff were the first to perform a mathematical analysis of the water coning problem and discovered the rate-sensitive behavior. They considered a horizontal, partially penetrated and homogenous sandstone reservoir with a hydrostatic pressure distribution. Initially, the water zone lies, due to its higher density, below the oil pay zone. Considering the imbalance of viscous and gravitational forces, they presented the following formula which became the main criterion for cone development.

$$\left(\frac{dp}{dr}\right)_{r=r_c} > (\rho_w - \rho_o) g cos\theta \quad (1)$$

where p is pressure, r is the radial distance around the wellbore, as shown in Figure 2, ρ_w is the density of water, ρ_o is the density of oil, g is the acceleration of gravity, and θ expresses the inclination of the fault (90° - the fault dip) that is considered (also shown in Figure 2).

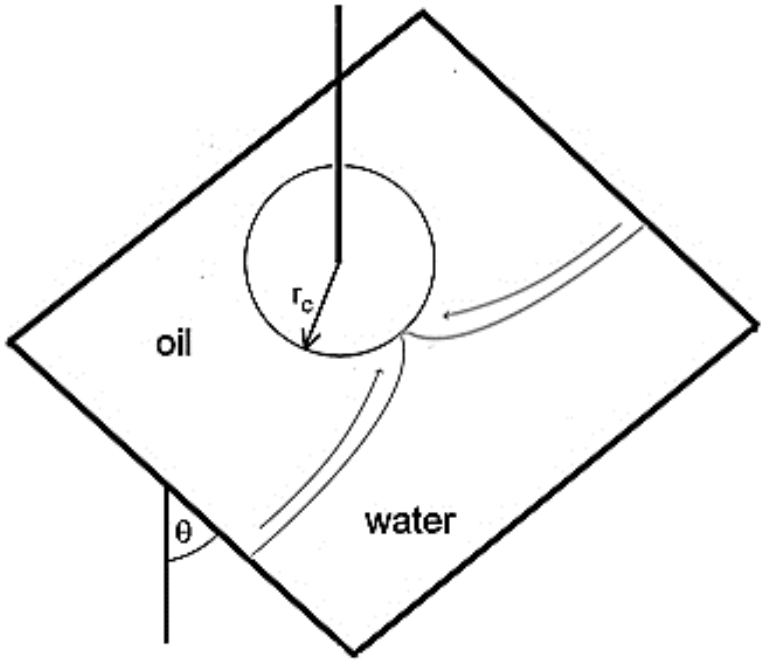

Figure 2 - Illustration of the critical radius for water coning.

Eq. 1 shows that if the viscous forces due to an applied pressure gradient (left term) exceed the gravitational forces (right term) a crest shaped oil-water contact is formed if the oil-water contact is at a distance less than the critical radius r_c below the well. Muskat and Wyckoff determined an appropriate maximum water free production rate for a partially penetrating well by solving single-phase, incompressible flow Laplace equations. Assuming a uniform-flux boundary condition at the well and neglecting the influence on the potential distribution by the cone shape, they concluded that the movement of the oil-water contact is directly proportional to the applied pressure gradient. Also with decreasing perforation length, the critical rate is expected to be higher. About 20 years later, Arthur (1956) investigated the problem of fingering and coning of water and gas in a homogenous oil sand and delivered a graphical solution for this problem based on Muskat's and Wyckoff's equation. To analyze the coning behavior in different reservoir geometries, Chaney et al. (1956) developed various curves for critical rate estimation based on the potentiometric model technique. A potentiometric analyzer basically uses the analogy between steady-state flow in a porous medium and the flow of electrical current in a conduit to estimate the potential function. The latter describes the relationship between the critical rate and dimensionless parameters defining

the system geometry. Chierici and Ciucci (1964) used a potentiometric analyzer to determine the dimensionless potential at the top of the cone and to compare the estimated critical coning height with Muskat's approximation. Just as Chaney et al. (1956), they obtained a smaller difference of about 15 percent and also presented a set of diagrams for the critical rate and the position and length of the perforation interval.

Sobocinski and Cornelius (1965) proposed a simple method to predict cone height and water breakthrough time for a given production rate. In their laboratory experiments they injected water into a wedge-shaped Plexiglas model filled with unconsolidated sand and simulated production by using an artificial lift system. At the outer boundary of the model oil and water were reinjected at a rate which maintains a constant level of the oil-water contact. With this method they derived the following equation for the dimensionless water cone height:

$$Z = 1.3055 \cdot 10^{-10} \frac{(\rho_w - \rho_o) k_h h(h - h_p)}{\mu_o B_o Q_o} \tag{2}$$

where ρ_w is the density of water, ρ_o is the density of oil, k_h is the horizontal permeability, h is the height of the oil column, h_p is the perforated interval, μ_o is the oil viscosity, B_o the formation volume factor and Q_o is the given oil production rate.

For the dimensionless breakthrough time:

$$t_{DBT} = \frac{4Z + 1.75Z^2 - 0.75Z^3}{7 - 2Z} \tag{3}$$

And for the exact prediction of time to water breakthrough:

$$t_{BT} = \frac{20325 \mu_o h \phi t_{D_{BT}}}{(\rho_w - \rho_o) k_v (1 - M^{\alpha})} \tag{4}$$

where ϕ is porosity, t_{DBT} is the dimensionless breakthrough time, k_v the vertical permeability and α is a coefficient which depends on the mobility ratio M ($\alpha = 0.5$ for $M < 1$ and $\alpha = 0.6$ for $1 < M < 10$).

In the 1970s various authors started to investigate coning, based on Muskat and Wyckoff's findings, in more complex reservoir geometries with the help of numerical simulations: To simulate water coning in a cylindrical reservoir domain, MacDonald (1970) employed three different numerical methods: The implicit pressure-explicit saturation (IMPES) formulation, a second method which considers the transmissibilities between the blocks to be implicit in the saturation equation and a fully implicit model. MacDonald studied the change of water saturation in the lower producing block and also the producing water-oil ratio over time for each model. He concluded that the fully implicit model is the most suitable one for the case of high capillary pressure values and small grid spacing near the wellbore. He also compared computing efficiency and truncation errors between the models. In 1971, Bournazel and Jeanson used experimental correlations and the Sobocinski-Cornelius experiment with a different determination of the dimensionless time to investigate isotropic, as well as anisotropic reservoirs with a lateral drive. Their work resulted in approximate values for critical rate and breakthrough time, but also in an evaluation of water-oil ratio over time. Similar to Bournazel and Jeanson's approach, Schols (1972) contributed to the study of water coning by using a Hele-Shaw model (Hele-Shaw, 1898) consisting of two horizontal and parallel plates, parted by a small gap and filled with glass granulate to represent Stokes flow through a porous medium. The result of his study, obtained from his experiments and numerical simulation, was an empirical correlation for a fully penetrating well. Schols' equation for the critical rate yields lower values than the one by Muskat and Wyckoff and also takes into account the influence of the wellbore radius in contrast to previous publications:

$$q_{Dc} = \frac{1}{2\pi}\left[0.432 + \frac{\pi}{\ln\left(\frac{r_e}{r_w}\right)}\right]\left[1 - \left(\frac{b}{h}\right)^2\right]\left(\frac{r_e}{h}\right)^{-0.14} \tag{5}$$

where q_{Dc} is the dimensionless critical production rate, r_e is the drainage radius, r_w is the well radius, b is the length of the perforation interval and h is the oil column height.

In comparison with the previous approaches, Chappelear and Hirasaki (1976) created a correlation for a partially perforated reservoir which is not completed to the top and introduced an “effective radius” to account for vertical flow resistance.

In 1985, Wheatley published a theory in which he analytically determined the critical rate for partially penetrating wells and discussed the conflicting results of previous authors. He considered a homogenous reservoir with an upper impermeable barrier and the oil-water contact at the lower boundary of the domain. By using the potential function for radial flow (Eq. 5) and correcting it by applying a line source beneath the well to satisfy the boundary conditions, Wheatley presented his procedure to calculate the critical rate.

$$\phi = 2qln\left(\frac{r}{r_e}\right) \tag{6}$$

where ϕ is in this case the potential, r the radius of investigation, r_e the dimensionless drainage radius and q is the source strength defined by Eq. 7:

$$q = \frac{Q\mu}{4\pi k_h h} \tag{7}$$

where Q is the oil production rate, μ is the oil viscosity, k_h the horizontal permeability and h is the height of the oil column.

Wheatley discovered that Muskat and Wyckoff over-predicted the critical rate by neglecting the presence of the water cone and by ignoring the influence of the wellbore radius. Accordingly, the calculation of the pressure distribution in

the reservoir is not accurate enough and Wheatley's new theory delivers the highest accuracy of all analytical approaches.

In the 1980s horizontal drilling started to gain economic viability and proved to be advisable in reservoirs with water coning problems since a smaller pressure drawdown was required to achieve the same oil production rate. Chaperon (1986) compared the critical rate of horizontal with vertical wells and presented the following estimation for horizontal wells in anisotropic reservoirs.

$$q_c = 1.165 \cdot 10^{-17} \frac{k_h (h - h_p)^2}{\mu_o B_o} \Delta\rho q_c^* \tag{8}$$

where q_c is the critical rate, k_h is the horizontal permeability, h is the pay zone, h_p the perforation interval, μ_o is the oil viscosity, B_o is the oil formation volume factor, $\Delta\rho$ is the positive density difference between oil and water and q^*_c is the critical rate coefficient which was correlated by Joshi (1991) as follows:

$$q_c^* = 0.7311 + \frac{1.943h}{r_e} \sqrt{\frac{k_h}{k_v}} \tag{9}$$

where r_e is the external drainage radius and k_v is the vertical permeability.

In contrast to the previous formulas, Eq. 8 and Eq. 9 show the major importance of the permeability ratio in reservoirs drilled with horizontal wells. Since in this case pseudo-radial flow occurs, also the vertical permeability needs to be considered in the calculations. Chaperon indicated that with increasing horizontal transmissivity and pay zone thickness the critical rate increases and decreases with increasing external drainage radius. Also Karcher et al. (1989) determined analytically the critical flow rates for horizontal wells in the cases of lateral edge drive (water inflow from the side boundaries of the reservoir), gas-cap drive and bottom water drive.

Instead of assuming a uniform flux at the wellbore like in Muskat's approach, Høyland (1989) used an infinitely conductive, vertical well in an anisotropic, homogenous reservoir for his analytical solution of the critical rate. Since he neglected the presence of the cone in the calculation of the pressure distribution, the results are similar to Muskat's approach, but Wheatley's results are within the 4% uncertainty lower. Høyland also applied a high number of numerical simulations to develop a correlation for different dimensionless wellbore radii and penetration depths.

In 1992, Guo and Lee discovered that the vertical pressure gradient below the perforations allows to estimate the existence of an unstable water cone. This gradient decreases with increasing radial distance from the well, resulting in a cone-shaped arrangement of points at which the dynamic and gravitational forces are in balance. Therefore, also the height of the oil-water contact is decreasing with radial distance and the typical cone-shaped structure is formed. Van Golf-Racht (1994) compared the coning behavior in a fractured reservoir with previous studies done on porous formations. He used five cases with varying pay zone thicknesses to determine the water-cut during production, the role of partial penetration and the importance of reservoir anisotropy. He concluded that Muskat's maximum water-free production rate in a porous medium is the same as the critical rate with a water-cut of zero in a naturally fractured reservoir. Van Golf-Racht expected that the critical rate is controlled by the same forces in both reservoir types.

Menouar and Hakim (1995) pointed out that in most cases the critical rate is treated as an increasing function of the anisotropy ratio (k_v/k_h). Meaning that with increasing vertical permeability, the vertical pressure gradient decreases and a higher critical production rate can be obtained. Menouar and Hakim concluded that this is only true for reservoirs with an anisotropy coefficient (the square root of the anisotropy ratio) between 0.5 and 1. For anisotropy coefficients between 0.01 and 0.1, e.g. reservoirs with thin barriers, the critical rate decreases with the coefficient. This strongly contrasts with Chaperon's conclusions which state that the vertical permeability should have just a minor influence on the critical production rate of horizontal wells.

Beattie and Roberts (1996) studied water coning in naturally fractured gas reservoirs with a bottom-water drive model. They varied different parameters (e.g. aquifer size, matrix and fracture permeability, fracture spacing etc.) to estimate their influence on breakthrough time, cumulative water production and ultimate gas recovery. Similarly to Van Golf-Racht, they concluded that these parameters have comparable effects on water coning in single porosity and fractured reservoirs. But like Menouar and Hakim, they stress the importance of the vertical permeability considering the cone development. To eliminate the assumption of segregated flow, Johns et al. (2002) studied the importance of capillary pressure and relative permeabilities for gas or water coning problems. Starting from Dupuit's equation (1863), they derived a steady-state analytical solution for a single well in an infinite-acting reservoir, assuming a constant free-water-level at a certain distance and vertical equilibrium. Vertical equilibrium of fluids, hydrostatic pressure gradient in the vertical direction, results in maximum crossflow and is realistic in reservoirs with increased vertical permeability and small oil column height. They studied the significant influence of the Bond number (ratio of buoyancy to capillary forces) on the critical rate in single and multiphase flow. An extension of this work was done by Ansari and Johns (2006). They developed analytical solutions using the principle of superposition for multiple wells and boundary conditions in a horizontal reservoir with constant thickness. Using different scenarios, they concluded that there is just a minor difference between their analytical and numerical solutions for aspect ratios greater than 10.

2.2 Literature Review on Inertial Effects in Factures

Significant research on inertial effects on flow in petroleum formations, especially in naturally fractured reservoirs, was done by different authors and is part of this section of the literature review. Additional information is also provided in the methodology section.

In 1995, Fourar and Bories conducted two-phase flow experiments in which they injected water and air into artificial horizontal fractures to measure the pressure drop and liquid flow fraction at steady-state conditions. They applied two different setups: the first setup used perfectly parallel glass plates and the second setup bricks which were made out of clay. By increasing the flow rate they obtained different flow regimes like bubble, fingering bubble, complex, annular and droplet flow. Fourar and Bories concluded that these flow regimes are comparable to those in tubes. Therefore, they modified Delhaye's method (1981) for multiphase flow in pipes to the two-phase flow in fractures and achieved similar results like in the experiments. Additionally, they applied the comparable Lockhart and Martinelli model (1949). An expression for the liquid volume fraction S_L as function of the Martinelli parameter X was obtained and resulted in a good match with the laminar flow experiments:

$$S_L = \left(\frac{X}{1+X}\right)^2 \tag{10}$$

with the Martinelli parameter:

$$X = \sqrt{\frac{\mu_L V_L}{\mu_G V_G}} \tag{11}$$

where μ and V are the viscosity and superficial velocity of the liquid phase L and gas phase G.

This study was continued by Fourar and Lenormand (2000) where they compared three different approaches with experimental results. The first one was the inertial factor model which applies the Forchheimer equation (Forchheimer, 1901). Together with their second one, the relative passability model, which is mainly used in nuclear engineering applications, the inertial and viscous terms are treated separately in the equation. This is contrary to the third approach, the Lockhart and Martinelli Model. It does not contain the concept of relative permeabilities and examines viscous and inertial effects globally.

Fourar and Lenormand concluded that the relative permeabilities are besides the saturation also a function of the flow rate ratio. A comparison of the inertial factor and the passability model with the experimental results shows a good match, but both approaches require a correlation or experimental determination of the relative permeability and passability. However, the benefit of the Lockhart-Martinelli model is that just two instead of four fitting parameters are needed, resulting in minor deviations within 20% from the experiments.

Continuing their research, Fourar et al. (2005) studied the effects of high velocity flow through a heterogeneous reservoir. In their study, they determined the dimensionless inertial coefficient β in the following equation by Forchheimer for serial-layers, parallel-layers and a correlated media that uses different correlation lengths:

$$\frac{dp}{dx} = -\mu \frac{Q}{A_c k}(1 + \beta R_e) \tag{12}$$

where p is the pressure, x the direction of flow, μ is the viscosity of the fluid, Q the flow rate, A the cross-sectional area of flow, k the intrinsic permeability, β the effective inertial coefficient and R_e is the Reynold's number.

A streamline simulator was used to calculate the flow rates and the Reynold's number in each grid block. By using the following equation, it was possible to determine the equivalent permeability of each grid block depending on the flow velocity:

$$k_e = \frac{k}{1 + \beta_0 R_e} \tag{13}$$

where k_e is the equivalent permeability and β_0 is the uniform inertial coefficient.

Afterwards, another simulation run which includes the new permeability was performed and the obtained pressure field was compared with the previous result. The process was repeated until no significant change in pressure was examined anymore, leading to a constant flow rate in the medium. After increasing the applied differential pressure, Fourar et al. determined the effective inertial coefficient from a plot of Δp versus Q.

They showed that the inertial coefficient is independent of the Reynold's number in the serial-layered model, but strongly affected in the case of parallel layering and the correlated model. Further results indicate that β increases with increasing variance and permeability ratio in the first case and decrease using the latter cases.

Brush and Thompson (2003) generated random rough-walled fracture models to analyze three different simulation approaches: full Navier-Stokes simulations, Stokes simulations and local cubic law governed simulations (detailed description is given in the methodology section). Using a finite volume discretization scheme they simulated flow through parallel-plate and sinusoidal fractures and compared the results with previous publications. Their main scope was to evaluate the validity of the local cubic law. Results showed that the flow rate in the Stokes simulations were within a range of 10% of the local cubic law simulations. However, this applied only to flow with a Reynold's

number smaller than 1 and low values of relative roughness and aperture of the fracture.

Another experiment on air and water flow through a fracture was done by Nowamooz et al. (2009). At first they measured the steady-state pressure drop in single-phase flow to determine the intrinsic permeability and cross-sectional area of the fracture.

In their two-phase model Nowamooz et al. applied the full cubic law including the F function (Fourar and Lenormand, 2000) which considers the second present fluid and is a function of the saturation of the fluid:

$$-\frac{\Delta p}{L} = \frac{\mu_l}{k}\left(F_l \frac{q_l}{A}\right) + \rho_l \beta \left(F_l \frac{q_l}{A}\right)^2 + \frac{\gamma q_l^2}{\mu_l}\left(F_l \frac{q_l}{A}\right)^3 \quad (14)$$

$$-\frac{\Delta p}{L} = \frac{\mu_g}{k}\left(F_g \frac{q_g}{A}\right) + \rho_g \beta \left(F_g \frac{q_g}{A}\right)^2 + \frac{\gamma q_g^2}{\mu_g}\left(F_g \frac{q_g}{A}\right)^3 \quad (15)$$

where Δp/L is the pressure drop per unit length, μ the viscosity, k the permeability, F the multiphase factor as a function of saturation, q the flow rate, A the cross-sectional area, ρ the density, β the Forchheimer inertial term and γ is an experimentally determined inertial parameter for the cubic term. The subscripts indicate the liquid phase l or gas phase g.

By increasing the air injection stepwise, they obtained the relative permeabilities for three different Reynold's numbers (0.07, 0.29 and 0.45) of the liquid phase. Each time the Reynold's number was increased also the pressure drop increased non-linearly, indicating the influence of inertia.

Chapter 3

Methodology

3.1 Governing Equations

Navier-Stokes Momentum Equation

In 1845, Stokes formulated a set of differential equations to describe the movement of liquids and gases through an open channel. This set describes the relationship between changes in the momentum of the fluid and the applied pressure gradients as well as viscous forces. The acceleration of a fluid particle can vary with time and space and is indicated by the left-hand side of the Navier-Stokes equation. The right-hand side of the formula represents the influence of external, internal and body forces.

Fluid density is assumed to be independent of pressure and the flow is considered as incompressible. Also, a Newtonian fluid with a constant viscosity is assumed so that the shear stress is linearly proportional to the applied strain rate.

The Navier-Stokes equation for incompressible flow of a Newtonian single phase fluid in vector form is:

$$\rho\left(\frac{\partial \boldsymbol{u}}{\partial t} + \boldsymbol{u}\cdot\nabla\boldsymbol{u}\right) = -\nabla p + \mu\nabla^2\boldsymbol{u} + \boldsymbol{F} \qquad (16)$$

where ρ is density, **u** is the fluid velocity vector, t is time, p is pressure, μ is viscosity and **F** is the body force vector (per unit volume) acting on the fluid.

Continuity Equation

The conservation of mass is represented by the continuity equation and necessary to get a closed system of equations in combination with the Navier-Stokes formula (c.f., Zimmerman & Bodvarsson, 1996). Since incompressible flow is assumed (dead oil and water), the conservation of mass is equivalent to the conservation of volume:

$$\nabla \cdot \boldsymbol{u} = 0 \tag{17}$$

The continuity equation states that the outflow rate must equal the inflow rate, since there is no accumulation of mass in the domain. Therefore, the divergence of the flow vector equals zero.

No-slip boundaries imply that the fluid velocity equals zero at the borders of the domain. This applies to the normal as well as to the tangential component of the velocity vector (Batchelor, 1967).

3.2 Conceptual model

It is assumed that the fluid flow occurs in a vertical, geological fault which is large in lateral and vertical extent, but just a few centimeters thin. In both scenarios, the naturally fractured basement and the clastic reservoir, the fault contains an oil column height of some hundred meters which is underlain by water. In the center of the fault, several meters above the oil-water contact, a horizontal well completion with a typical radius was set for production at a constant rate. The fault is fully penetrated by this well and wellbore storativity and skin effect were neglected. Since the whole wellbore-surface was considered to be open to fluid inflow, this setup is equivalent to an open-hole completion. The oil and water phase are assumed to be incompressible, therefore oil and water can enter the fault at a rate which equals the outflow at

the well. At a production above the critical rate, an inflow of water into the well is expected since the cone becomes unstable. However, at a sufficient lateral distance from the well the oil-water contact is supposed to stay constant at its initial level where no pressure perturbation by the well is assumed.

3.3 Model setup

A two-dimensional fault model, as shown in Figure 2, was used for the analytical calculations and constructed in CAD for numerical simulations. The fault was treated as zone with laminar Darcy flow in one case and with Forchheimer flow in the other case. The model is 2,000 m in width, 600 m in height and due to the 2D simulation assumptions, a thickness of 1 cm was used for volumetric calculations in the open conduit simulation. The oil column is 330 m and the water column 270 m high. The distance between the horizontal well and the oil-water contact was set to 30 m. An infinite-conductive well was assumed, a wellbore radius of 0.15 m chosen and the outflow rate varied to determine the critical production rate.

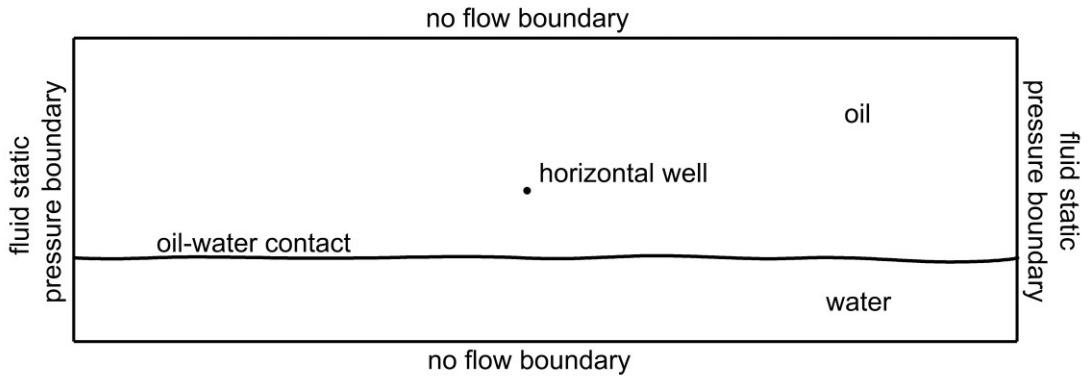

Figure 3 - Fault model with a horizontal well in the centre.

Oil and water can flow through the left and right boundary into the domain. However, fluid static pressure boundaries were applied at the left and right side and no-flow barriers were imposed at the top and the bottom of the domain.

3.4 Analytical solution

3.4.1 Faults in naturally fractured reservoirs

This section provides an analytical solution derived by using Muskat's equation (1935) to determine the critical rate at which water coning occurs in a theoretical, brittle and single-fracture type fault model. Several assumptions and simplifications were made to develop a simple formula for the proposed problem by following the analysis by Zimmerman and Bodvarsson (1996).

Recalling the Navier-Stokes equation:

$$\rho\left(\frac{\partial \boldsymbol{u}}{\partial t} + \boldsymbol{u}\cdot\nabla\boldsymbol{u}\right) = -\nabla p + \mu\nabla^2\boldsymbol{u} + \boldsymbol{F} \tag{18}$$

where ρ is density, **u** is the fluid velocity vector, t is time, p is pressure, μ is viscosity and **F** is the body force vector (per unit volume).

The body force vector **F** considers other external forces, in this case gravity, and can be expressed in the following way by acknowledging that the z direction is positive upwards:

$$\boldsymbol{F} = \begin{pmatrix} 0 \\ 0 \\ -\rho g\nabla z \end{pmatrix} \tag{19}$$

where g is the acceleration due to gravity with a value of 9.81 m/s^2.

For simplicity reasons, steady-state flow is assumed and inertial effects are neglected. As a result, the left-hand term vanishes and the equation is reduced to Stoke's linear creeping flow equation:

$$\mu \nabla^2 \boldsymbol{u} = \nabla p + \boldsymbol{F} \tag{20}$$

At this point, a vertical, perfectly parallel plate model is taken into account. Considering that the pressure gradient lies only in the vertical direction and therefore flow results in the opposite direction, it is possible to express Eq. 14 in the following way:

$$\frac{\partial^2 u_z}{\partial x^2} = \frac{1}{\mu}\frac{\partial p}{\partial z} - \rho g \tag{21}$$

Since the plates are stationary and represent no-slip boundaries, the flow velocity at the upper and lower boundary also equals zero.

After integration the following result is obtained:

$$u_z(x) = \frac{1}{2}\left(\frac{1}{\mu}\frac{dp}{dz} - \rho g\right)\left[x^2 - \left(\frac{b}{2}\right)^2\right] \tag{22}$$

where b is the gap between the plates or the aperture of the fracture.

Additionally, the total flow rate Q is determined by integration of Eq. 16 across the fracture aperture and multiplication with the fracture width w:

$$Q = \frac{1w}{2}\left(\frac{1}{\mu}\frac{dp}{dz} - \rho g\right)\int_{-b/2}^{+b/2}\left[x^2 - \left(\frac{b}{2}\right)^2\right]dx \tag{23}$$

$$Q = -\frac{wb^3}{12\mu}\left(\frac{dp}{dz} - \rho g\right) \tag{24}$$

By assuming that this approximation is valid for fracture flow, the fracture permeability, Eq. 18 can be rewritten in the following form which is identic to Darcy's law (Darcy, 1856):

$$Q = -\frac{k_f A}{\mu}\left(\frac{dp}{dz} - \rho g\right) \tag{25}$$

with k_f as the permeability of the fracture:

$$k_f = \frac{b^2}{12} \tag{26}$$

And A the cross-section area of the fracture:

$$A = wb \tag{27}$$

Eq. 18 is also known as the "cubic law" and is valid for perfectly parallel, smooth walled plates (Hele-Shaw, 1898). Due to the wall-roughness and variation of hydraulic aperture of natural fractures and faults, the application of this law has only limited success and is often corrected with the use of various correlations and experimental studies.

Since the producing well causes circular equipotential lines of pressure to develop, the cross-sectional area of the fracture needs to be replaced by the cylindrical cross-sectional area of flow:

$$A_c(r) = 2\pi rb \tag{28}$$

Additionally, the focus lies on the flow of the oil phase in a two-phase flow regime and thus, oil formation volume factor B_o and oil viscosity μ_o need to be introduced. By also neglecting the effects of capillary pressure Eq. (18) results in:

$$Q = -\frac{2\pi rb^3}{12\mu_o B_o}\left(\frac{dp}{dr} - \rho_o g\right) \tag{29}$$

Another important aspect that has to be considered is the present flow regime. If the Reynold's number exceeds a certain value (usually between 2300 and 4000), turbulent fluid flow can be expected. Since Darcy's law is only valid for slow, viscous flow (Reynold's number smaller than 1), a constant inertial term is added to Eq. (23). This term is referred to as the Forchheimer correction term β (Forchheimer, 1901) and is used to account for the non-linear relationship between the pressure gradient and velocity.

By rearranging Eq. (23) and adding the inertial term, the hydrodynamic gradient can be expressed as:

$$\frac{dp}{dr} = -\frac{6Q\mu_o B_o}{\pi rb^3} + \rho_o g - \beta\rho_o B_o\left(\frac{Q}{2\pi rb}\right)^2 \tag{30}$$

where β is the Forchheimer correction term or inertial resistance and ρ_o is the density of the oil phase.

As mentioned earlier, a water crest will evolve with its tip at the critical distance vertical to the wellbore, if the hydrodynamic gradient exceeds the gravity gradient as the production rate is increased. Recalling the criteria for coning by Muskat and Wyckoff with the necessary adjustments for a horizontal well in a vertical fault:

$$\left(\frac{dp}{dr}\right)_{r=r_c} > (\rho_w - \rho_o)gcos\theta \tag{31}$$

where ρ_w is the water density and θ the inclination of the fracture plane.

Inserting the hydrodynamic gradient into Muskat's equation:

$$-\frac{6Q\mu_o B_o}{\pi r b^3} + \rho_o g - \beta\rho_o B_o \left(\frac{Q}{2\pi r b}\right)^2 > (\rho_w - \rho_o)gcos\theta \tag{32}$$

Since the oil-water contact is perpendicular to the vertical axis of the domain, the inclination equals zero and the critical radius or critical length can symbolized as the critical vertical distance z_c.

The previous equation can be rearranged to find z_c. The latter is the minimum distance between the well and the oil-water contact to prevent coning at a given flow rate Q and a constant inertial term β:

For a turbulent flow regime:

$$z_c = \frac{1}{2}\frac{\left[6\mu_o B_o + \sqrt{B_o(36\mu_o^2 B_o + 2\beta{\rho_o}^2 b^4 g - \beta g\rho_o\rho_w b^4)}\right]Q}{\pi g b^3(2\rho_o - \rho_w)} \tag{33}$$

And for laminar flow (β=0):

$$z_c = \frac{6Q\mu_o B_o}{\pi g b^3 (2\rho_o - \rho_w)} \tag{34}$$

The more practical method is to determine the critical rate Q_c at a given distance z between the fluid interface and the horizontal well. In this case the coning criteria for turbulent flow is expressed in the following way.

$$Q_c = -\frac{2\pi z\left[6\mu_o B_o - \sqrt{B_o(36\mu_o^2 B_o + 2\beta {\rho_o}^2 b^4 g - \beta g \rho_o \rho_w b^4)}\right]}{\beta \rho_o B_o b} \tag{5}$$

For laminar flow:

$$Q_c = \frac{\pi g z b^3 (2\rho_o - \rho_w)}{6\mu_o B_o} \tag{36}$$

3.4.2 Faults in clastic reservoirs

In this section an analytical solution for a vertical fault model in a homogenous, isotropic sandstone reservoir is presented by adjusting the derivation of the previous section in just a minor way: Since conductive fractures are absent, the flow occurs through the pore network of the formation and is therefore controlled by the porosity and the permeability of the matrix. In this case, the permeability of the fault depends on various factors like fault displacement, cataclasis and diagenesis. Various author, for example Manzocchi (1999) and Sperrevik (2002), provided empirical correlations of fault rock properties. In this derivation, a constant value for permeability and a laminar flow behavior is assumed.

Starting with Darcy's equation for laminar flow through a pore network:

$$\frac{dp}{dr} = -\frac{QB_o\mu_o}{2r\pi bk} + \rho_o g \tag{37}$$

In combination Muskat's coning criteria:

$$\left(\frac{dp}{dr}\right)_{r=r_c} > (\rho_w - \rho_o) g cos\theta \tag{38}$$

Resulting in a formula for the minimum distance z_c between the well and the oil-water contact to prevent coning at a given flow rate Q:

$$z_c = \frac{Q\mu_o B_o}{2\pi g b k(2\rho_o - \rho_w)} \tag{39}$$

Rearranging the equation results in a critical production at a given distance z between the well and oil-water contact:

$$Q_c = \frac{2\pi gbkz(2\rho_o - \rho_w)}{\mu_o B_o} \tag{40}$$

3.5 Numerical simulation

3.5.1 Governing equations

To verify the numerical scheme and to simulate two-phase flow through a permeable fault the commercial CFD software ANSYS Fluent was used to solve the conservation equations for mass and momentum.

Where the general conservation of mass or continuity equation is defined by:

$$\frac{\partial \rho}{\partial t} + \nabla \cdot (\rho \boldsymbol{u}) = S_m \tag{41}$$

where ρ is the fluid density, **u** the velocity vector and S_m is the mass source.

And recalling the conservation of momentum (Newton's second law) or Navier-Stokes equation:

$$\rho \left(\frac{\partial \boldsymbol{u}}{\partial t} + \boldsymbol{u} \cdot \nabla \boldsymbol{u} \right) = -\nabla p + \mu \nabla^2 \boldsymbol{u} + \boldsymbol{F} \tag{42}$$

where ρ is density, **u** is the fluid velocity vector, t is time, p is pressure, μ is viscosity and **F** is the body force vector (per unit volume) acting on the fluid.

In this study no heat transfer and compressibility is modeled and therefore the additional energy equation is not being solved during the simulation.

3.5.2 Discretization

The governing equations were discretized spatially by using the finite volume method which is considered as the appropriate method to solve advective equations. The computational domain needs to be divided into a specified number of control volumes. The center of each control volume or cell stores the necessary scalar values and interpolation schemes are used to determine the values at the cell faces. In this case, the PRESTO! (PREssure STaggering Option) method was chosen as the pressure interpolation scheme in the momentum equation. It can be used for flows with high swirl number, but is also recommended for multiphase flow problems in curved and porous domains. By using this scheme, pressure gradient assumptions and interpolation errors at the cell faces are minimized, resulting in a higher accuracy. As an unstructured mesh was used, the Least Squares Cell-Based Gradient Evaluation was utilized, since less computational effort is required.

In this thesis, a quad-dominant mesh with a maximum element size of 20 m was created with the use of ANSYS ICEM CFD, as shown in Figure 4. In the close proximity of the well the mesh size was reduced to a value of 0.1 m, since the highest velocities can be expected in this domain of the model. To model a sharp fluid interface, the borders of the cells were aligned parallel to the oil-water contact.

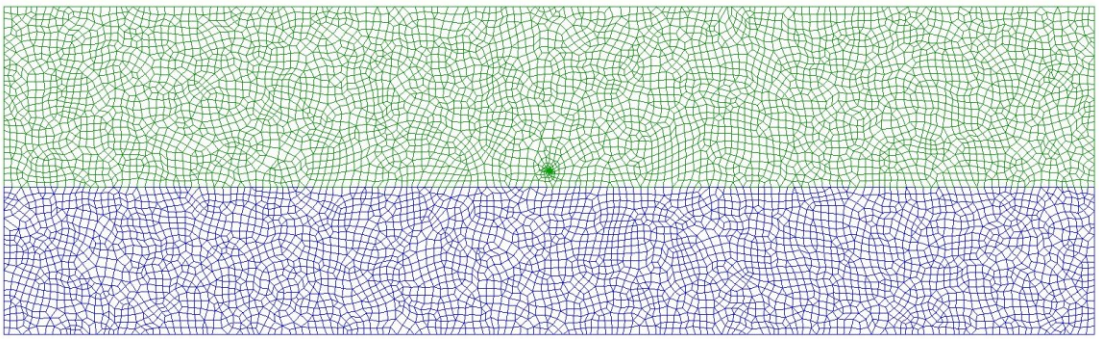

Figure 4 – Final, quad-dominant mesh with a cell alignment at the oil-water interface, a reduce cell size near the wellbore and total number of 9,103 elements.

For the time discretization a second-order implicit scheme was utilized and applied to all transport equations in the simulations. The VOF method requires that a pressure-based solver is chosen, which is mainly applied for low-speed incompressible flow problems through a domain. Further, an absolute velocity formulation was specified to reduce numerical diffusion since no transformation of the velocity at the interface between two subdomains is needed.

Since there is no independent equation for the pressure field during incompressible flow, a pressure-velocity coupling algorithm is required. In this case, the Pressure-Implicit with Splitting of Operators (PISO) (Issa, 1986) was chosen. An intermediate velocity field is calculated by solving the momentum equation to compute the mass fluxes at the cell faces. Afterwards, the continuity equation is reformatted to derive an additional condition for the pressure field to correct these face fluxes. Based on the new pressure field, also the velocity field is recalculated. This process is repeated a defined number of times before the remaining transport equations are solved.

3.5.3 Multiphase flow model

The multiphase flow was numerically calculated using the Euler-Euler approach which applies the concept of interpenetrating continua. It states that the volume of one phase cannot be occupied by another phase.

Therefore, the continuity equation is solved for the volume fraction α of each phase q in each cell:

$$\frac{1}{\rho_q}\left[\frac{\partial}{\partial t}\left(\alpha_q \rho_q\right) + \nabla \cdot \left(\alpha_q \rho_q \boldsymbol{u}_q\right) = S_{\alpha_q} + \sum_{p=1}^{n}\left(\dot{m}_{qp} - \dot{m}_{pq}\right)\right] \qquad (43)$$

where $\dot{m}_{qp}$ is the transfer of mass from phase q to phase p and $\dot{m}_{pq}$ the reverse process.

To track the interface between the oil and water phase the Euler-Euler Volume of Fluid (VOF) model was used. The VOF method was first of all applied by Hirt & Nichols (1979) to track free fluid surfaces in a fixed Eulerian mesh.

Therefore, the VOF method is especially applied in simulation where the focus lies on the position of the interface between fluids. At each time step a single set momentum equation is solved and the volume fraction of each fluid is tracked to compute the interface. Their sum must always equal one. Additionally, a volume fraction equation with geometric reconstruction interpolation scheme was chosen, to obtain an even sharper oil-water contact.

Hirt & Nichols (1979) stated that the volume fraction can either represent a cell fully saturated by only one phase or by a mixture of fluids:

Volume Fraction α	Meaning
0	the cell is empty of fluid i
1	the cell is completely filled with fluid i
0 < Ci < 1	a mixture of fluid i and one or more other fluids and the interface are present

Table 1 - Volume fraction variables for the VOF model

3.5.4 Numerical model setup

Also in the simulations an incompressible, Newtonian fluid was applied and the number of mass transfer mechanisms set to zero since no mass exchange between the two phases is expected. Further, the surface tension force was neglected too.

The chosen parameter values for average oil and water densities and viscosities are shown in Table 2 and are also consistent with industry standards and fluid properties found in a high number of hydrocarbon reservoirs all over the world.

	Primary Phase	**Secondary Phase**
Property	**Oil**	**Water**
Density [kg/m^3]	850	1,000
Viscosity [Pa s]	0.005	0.001
Formation Volume Factor [m^3/sm^3]	1.0	1.0

Table 2 – Oil and water properties set in the simulation runs.

3.5.5 Boundary conditions

Various simulations with constant pressure at the bottom-boundary were run to simulate a bottom water drive, but results showed that at a certain production rate the oil-water contact moved rapidly upwards, maintaining a horizontal shape of the interface instead of developing a cone.

Since that kind of production behavior is rather unrealistic, the top and the bottom boundaries were treated as no-flow barriers/walls to prevent inflow at these locations.

Therefore, the side-boundaries were split into two parts. In the part above the oil-water contact only an influx of the oil phase is permitted (water volume fraction equals 0) and below the interface only water is entering the fault (water volume fraction is 1). Hence, the oil-water constant is kept at constant height at the sides of the domain, assuming that no pressure perturbation will affect the interface at such a large distance from the well.

Since it is not possible to specify a constant outflow rate at the well in the used software, a constant, negative velocity inlet was specified for the inner boundary condition. Multiplication of this outflow velocity with the cylindrical wellbore surface, resulted in the expected production rate.

Chapter 4

Results

4.1 Faults in clastic environments

In this section, the analytical and numerical results of a faulted sandstone reservoir with specified porosity and permeability are presented. For the determination of the critical rate the following additional reservoir parameters have been applied.

Property	Value
Fault Porosity	0.20
Fault Permeability	10^{-12} m^2

Table 3 - Fault properties for the case of a clastic environment.

Since it is assumed that the Reynold number in these scenarios never exceeds a value of 1, the equation for the critical rate for Darcy flow with isotropic permeability (Eq. 40) was used.

$$Q_c = \frac{2\pi g b k z (2\rho_o - \rho_w)}{\mu_o B_o} \tag{44}$$

$$\frac{2\pi \cdot 9.81 \cdot 0.01 \cdot 10^{-12} \cdot 30(2 \cdot 850 - 1000)}{0.005 \cdot 1} = 2.59 \cdot 10^{-6} \frac{m^3}{s}$$

Therefore, the analytical solution yielded an absolute value of $2.59 \cdot 10^{-6}$ m^3/s which equals approximately 1.4 barrels of oil per day. To illustrate the dependency of the critical rate on fault permeability and distance z, the following plot was constructed (Figure 5).

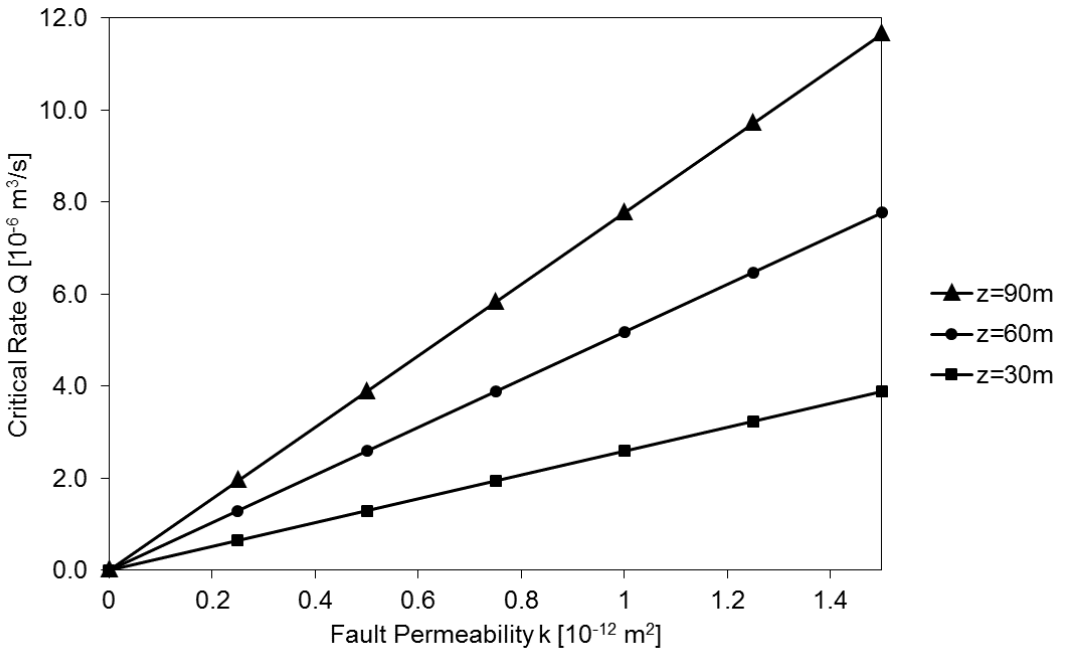

Figure 5 - Chart shows the critical rate as function of fault permeability for three different distances between oil-water contact and horizontal well.

A production rate of $2.59 \cdot 10^{-6}$ m^3/s equals a resulting well inflow velocity of $3 \cdot 10^{-4}$ m/s and was used as the input for the steady-state simulation. After several hundred iterations a solution was obtained, but a development of a water cone was not observed. The oil-water contact remained at its initial position and just the oil phase was produced, as shown in Figure 6.

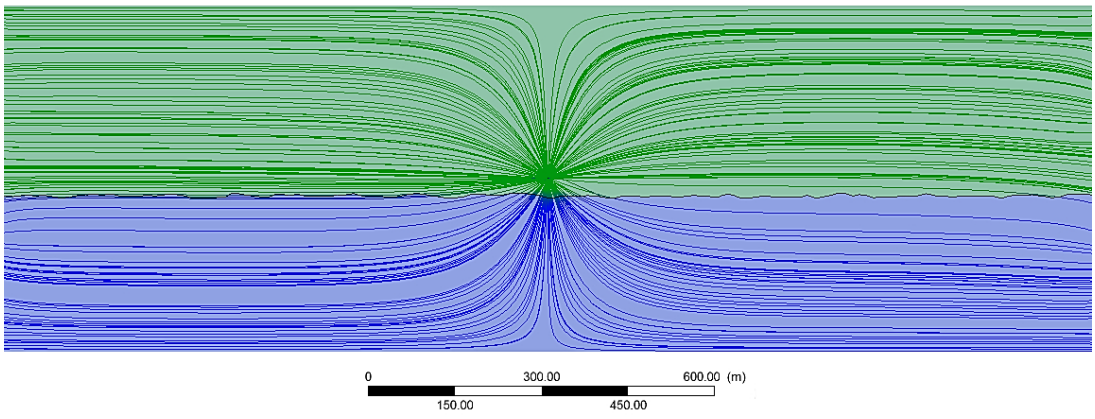

Figure 6 - Steady state simulation result with a constant production rate of $2.59 \cdot 10^{-6}$ m^3/s. The oil phase (green) and water phase (blue) are clearly separated by the horizontal fluid contact. The streamlines indicate that only oil had been produced and no water breakthrough had been obtained.

Figure 7 illustrates that the pressure disturbance is not strong enough to make any impact in the vicinity of the oil-water interface. With the current level of resolution of the interface, the pressure gradient does not exceed the hydrodynamic gradient and therefore no coning is observed.

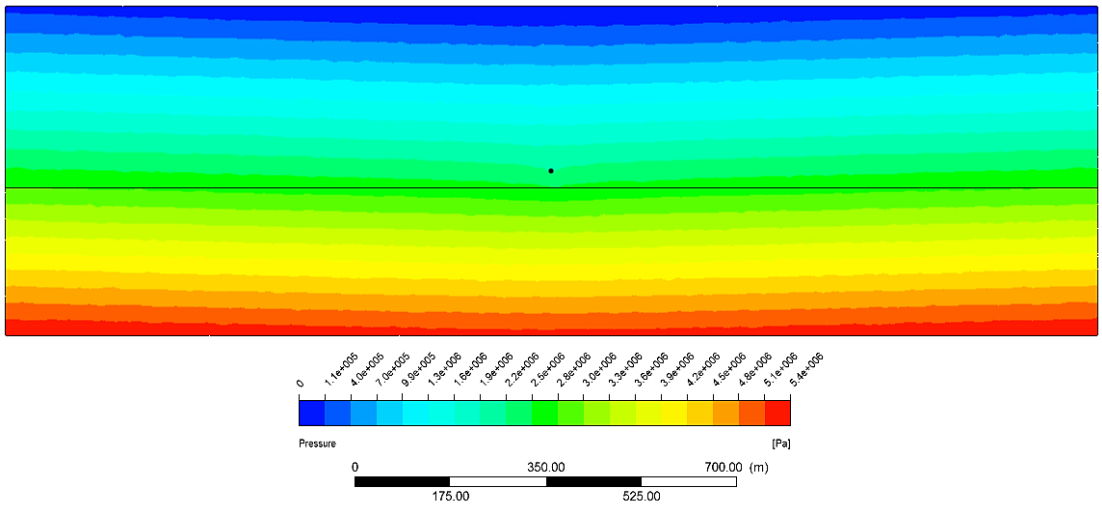

Figure 7 – Pressure contours showing just a minor bending of the contour lines around the well which is not significant enough to result in water coning.

To get water coning as a results of the simulations, the well inflow velocity and therefore the production rate was gradually increased. The first cone development was realized at an inflow velocity of 0.0012 m/s, which equals $1.13 \cdot 10^{-5}$ m^3/s (numerical critical rate) and water breakthrough at the well at 0.0013 m/s, equivalent to $1.23 \cdot 10^{-5}$ m^3/s, as shown in Figure 8 and Figure 9.

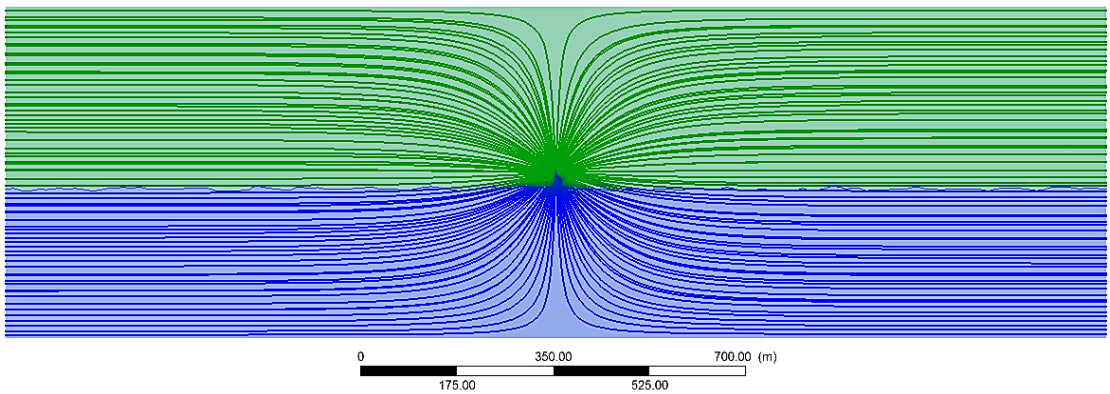

Figure 8 - Volume fraction contours and streamlines at a production rate of $1.23 \cdot 10^{-5}$ m^3/s. Coning and water breakthrough had been detected and therefore the critical rate determined.

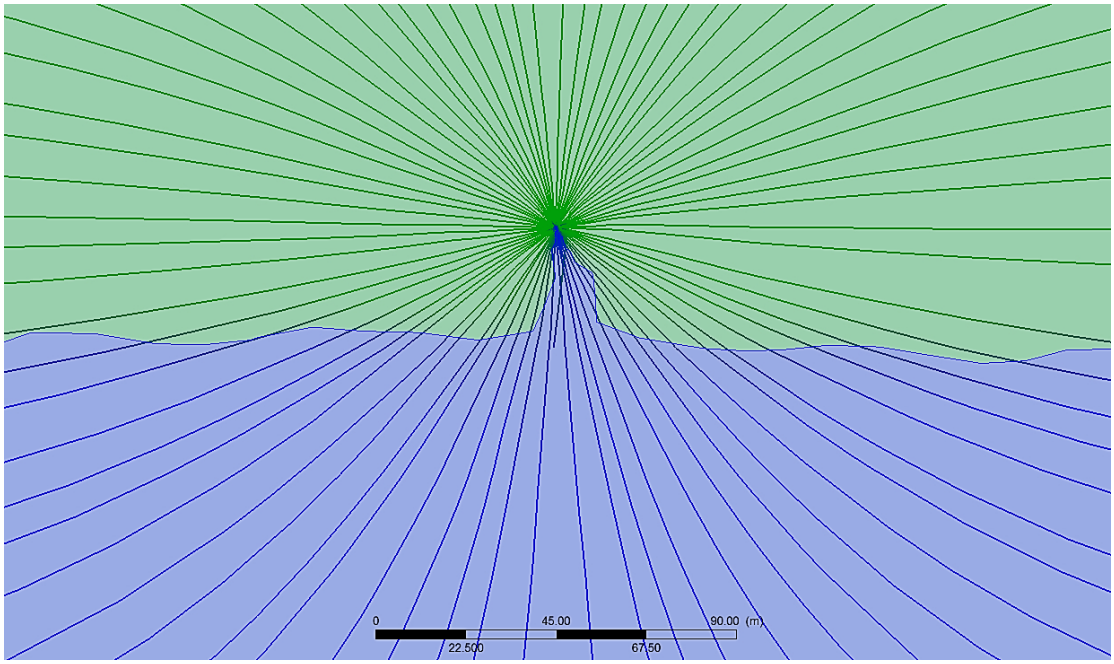

Figure 9 – Close-up view of the water cone resulting from the steady-state simulation for a fault in a clastic environment. The height of the cone was estimated to be about 25 m since the oil-water contact moved vertically upwards. Additionally, the importance of the interface resolution is illustrated.

Due to a higher production rate, the pressure perturbation affected the whole reservoir domain and radial occurs until the no-flow boundaries at the top and bottom of the reservoir affect the pressure distribution, as shown in Figure 10.

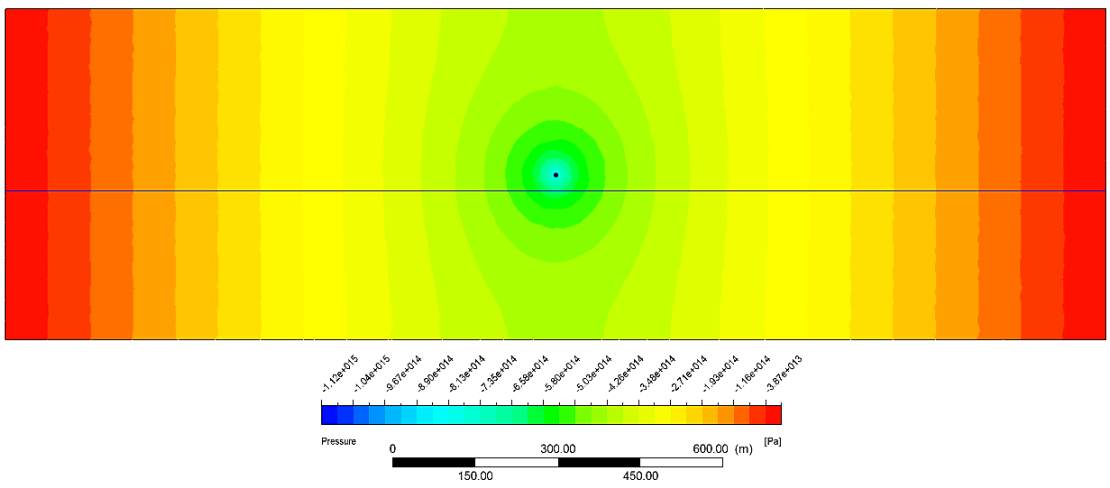

Figure 10 – Pressure distribution at water breakthrough. In the vicinity of the initial oil-water contact, represented by a horizontal line, the pressure contour lines are circular and a radial flow regime can be expected, also show by the streamlines in the previous figures.

4.2 Faults in naturally fractured environments

In this scenario a parallel plate model was assumed, representing a fault/conduit in a brittle, fractured basement reservoir rock. All the scenarios with varying inflow velocity resulted in a rather high Reynolds number and therefore inertial effects had to be considered. For both, the analytical and numerical determination, a constant inertial resistance β of 10^8 m^{-1} was applied.

For the analytical solution:

$$Q_c = -\frac{2\pi z\left[6\mu_o B_o - \sqrt{B_o(36\mu_o^2 B_o + 2\beta\rho_o{}^2 b^4 g - \beta g\rho_o\rho_w b^4)}\right]}{\beta\rho_o B_o b} \qquad (45)$$

$$= -\frac{2\pi\cdot 30\left[6\cdot 0.005\cdot 1 - \sqrt{1(36\cdot 0.005^2\cdot 1 + 2\cdot 10^8\cdot 850^2\cdot 0.01^4\cdot 9.81 - 10^8\cdot 9.81\cdot 850\cdot 1000\cdot 0.01^4)}\right]}{10^8\cdot 850\cdot 1\cdot 0.01}$$

$$Q_c = 5.36\cdot 10^{-4}\,\frac{m^3}{s}$$

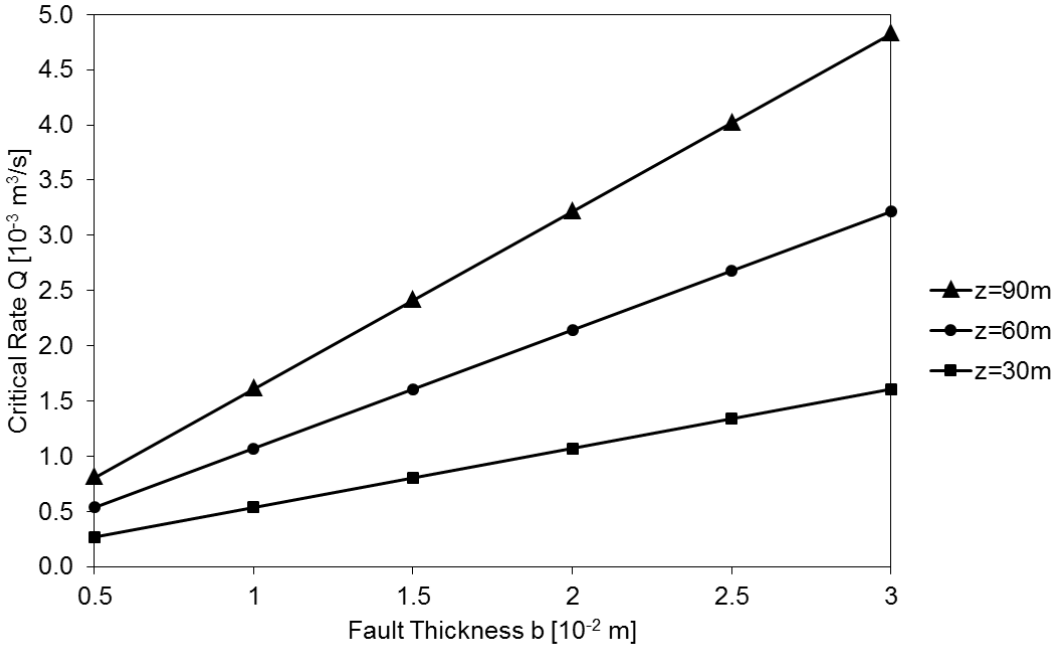

Figure 11 - Chart shows the critical rate as function of fault thickness for three different distances between oil-water contact and horizontal well.

The analytical critical rate resulted in an absolute value of $5.36 \cdot 10^{-4}$ m^3/s (290 bbl/day) and equals a well-flowing velocity of $5.68 \cdot 10^{-2}$ m/s. In the simulations, a stable cone development and water breakthrough was monitored. The streamlines in Figure 12 illustrate the turbulent flow behavior in the contrast to the equally spaced streamlines during laminar flow. The flow is restricted due to the inertial resistance and no uniform inflow into the horizontal well is shown.

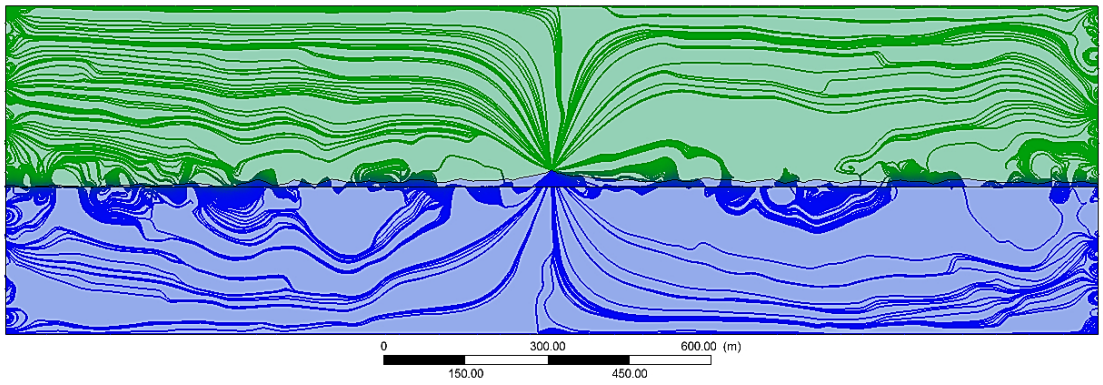

Figure 12 - Steady state simulation result for a vertical conduit with a constant production rate higher than the critical one.

Also in this case the deflection from a hydrostatic pressure distribution is minimal, as shown in Figure 13.

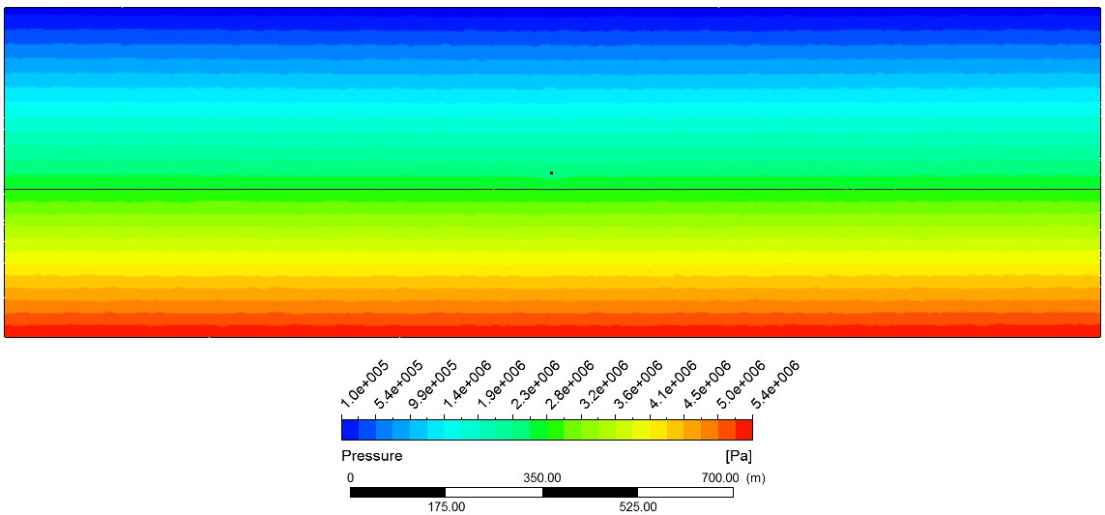

Figure 13 - Pressure distribution at the end of the simulation in the case of water coning in an open conduit.

In the sensitivity analysis the inflow velocity was gradually lowered and the result of the simulation was observed after each change of the production rate.

Using this procedure the production rate was determined at which coning and water breakthrough occurs in the simulation. Table 3 summarizes these steps and their results.

Scenario	Well-Inflow Velocity [m/s]	Production Rate [m^3/s]	Comments
1	**0.056**	**$5.36 \cdot 10^{-4}$**	**Analytically determined critical rate.**
2	0.025	$2.36 \cdot 10^{-4}$	Smaller cone around the wellbore with a shorter lateral extend.
3	0.015	$1.41 \cdot 10^{-4}$	Shrinking cone. Water still produced.
4	0.010	$9.42 \cdot 10^{-5}$	Production rate at which water breakthrough occurred.
5	**0.009**	**$8.48 \cdot 10^{-5}$**	**Numerically determined critical rate. (No water breakthrough)**
6	0.008	$7.54 \cdot 10^{-5}$	Stable cone developed, but no water breakthrough was observed.

Table 4 – Results of the different simulation scenarios for coning in a vertical conduit

With the simulations a critical rate of $8.48 \cdot 10^{-5}$ m^3/s, which equals around 46 barrels per day, was determined (Figure 14). Since the oil initially in place is approximately 42 barrels, the daily recovery factor would be around 0.1%.

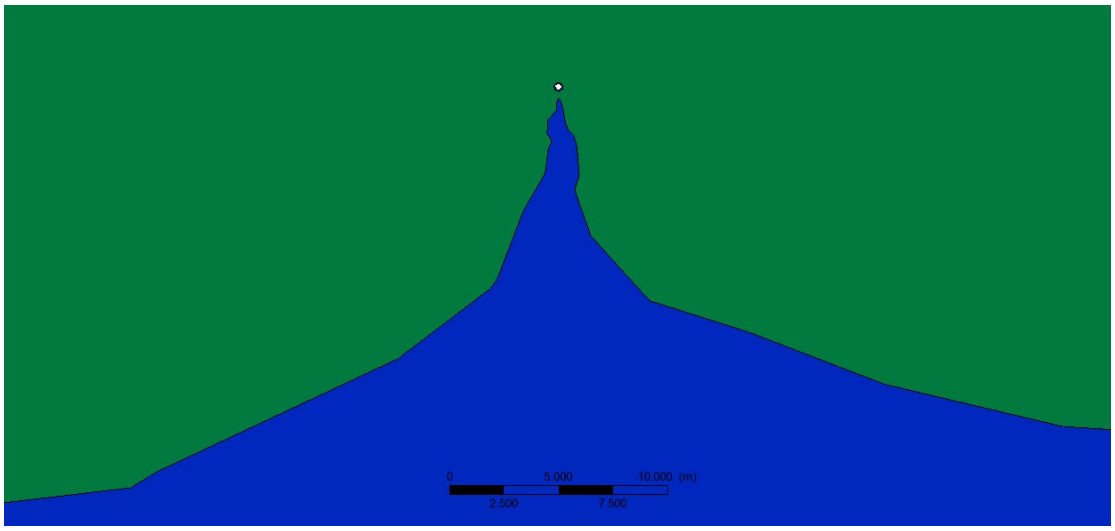

Figure 14 - Water coning in an open conduit at the critical rate before water breakthrough

Chapter 5

Discussion

The water coning behavior in vertical permeable faults in clastic and in naturally fractured reservoir was investigated analytically and numerically. To validate the numerical model, the results for the maximum water-free production rate (critical rate) were analyzed and compared. Depending on the reservoir type, the relative error between analytical and numerical determination is 0.8 and 3.3. This section provides my interpretations and opinion on the results.

5.1 Faults in clastic environments

Since only the flow through a porous fault zone with a small thickness was considered, the analytical and numerical solution for the critical rate resulted in very low values. Therefore, an economic production of the domain would not be feasible due to the minimal recovery rate.

Nevertheless, the conducted analysis shows that coning is strongly affected by different parameters, like the distance between the oil-water contact and the well, the permeability and the thickness of the fault. This replicates the findings of Chaperon (1986) and Menouar and Hakim (1995) in clastic reservoir formations drilled by vertical wells. However, since a horizontal well drilled into a vertical fault was investigated in this thesis, gravitational effects have a large impact on the flow behavior. Neglecting these effects would result in a higher hydrodynamic gradient and therefore in a much lower critical production rate.

Since the analytical approach does not address boundary effects, a comparison with the numerical solution is just possible if these effects are mainly eliminated in the simulations. Therefore, large distances between the well and the borders of the domain were chosen. However, the simulations showed that the critical rate does not increase linearly with increasing distance between the oil-water contact and the wellbore. This leads to the assumption that despite the large distances, effects from the impermeable top and bottom boundaries still have a minor influence on the fluid flow and reduce the critical rate. To correct this effect the principle of superposition would need to be applied. In the method of images (Bear, 2013) the production well is mirrored to the other side of the no-flow barrier. Both wells produce at the same rate and the individual flows are superposed, resulting in a solution that satisfies the no-flow boundary condition. Nevertheless, the error caused by neglecting the boundary effects is considered as insignificant in this study.

Considering a laminar flow regime in both solutions, a comparison between the analytically determined critical rate and the numerical one resulted in a low relative error of 0.8. The main reason which causes this deviation is probably the neglected influence of the water cone on the pressure distribution in the derivation of the analytical solution. An implementation of Wheatley's potential function for radial flow (1985) possibly corrects this error, but also results in a too high complexity in the analytical determination.

I am aware that this analysis fails to address capillary effects, wettability and the effects of relative permeabilities which have serious influence on the fluid flow through a porous network.

5.2 Faults in naturally fractured environments

Since the conductivity of brittle and empty faults in naturally fractured reservoirs is significantly higher, also the critical rate is higher than in the previous case. Due the application of the “cubic law” in the analytical solution a strong dependency on the fault thickness was recognized. Additionally, gravitational effects and the distance between the fluid contact and the well have a significant impact on the flow velocity inside the domain. By comparing the analytical approach based on Forchheimer dominated flow with the CFD simulation a relative error of 3.3 was obtained. Several possible reasons led to this deviation:

For the case of simplicity, the altered pressure distribution caused by the presence of the cone and boundary effects were again neglected in the analytical solution. Therefore, the critical rate was over-predicted and requires likewise the application of the method of images for correction.

The Forchheimer approximation has its limitations since it is only applicable to weak inertial flow. However, the simulation results show that strong inertial effects are present and turbulent flow is dominating. To account for these additional pressure loses, it would be necessary to solve full Navier-Stokes equations analytically, resulting in an unreasonable complexity.

In contrast to this thesis which uses a simple perfectly parallel-plate geometry, case studies of natural fractured basement reservoirs (e.g. in South East Asia) reveal more complex flow geometries. Especially in fracture networks with a large number of intersections, bends or variable apertures, the main direction of motion is changed, resulting in large pressure losses (Kosakowski and Berkowitz, 1999; Witherspoon et al., 1980).

When the fluid flows through a bended section an inward acceleration is caused by radially acting forces, resulting in a development of a pressure gradient from the outside to inside of the curvature (Chisholm, 1980). At the outer wall of the bend an increased pressure and lower fluid velocity is observed and in contrast, a lower pressure and higher velocity close to the inside wall. This effect is based on Bernoulli's law which states that the sum of potential, kinetic and internal energy remains constant (Bernoulli, 1738). The mentioned pressure gradient causes a flow separation and small eddies to form near the outer wall and the bend at the outlet branch. Depending on the bend angle, this leads to a further increase in pressure losses.

Additionally, secondary flows of the second kind (Prandtl, 1952; Gessner, 1973) which are perpendicular to the main flow direction in a non-circular cross-section can develop near constrictions of the conduit. Due to a higher flow velocity in these regions also a higher pressure gradient is required to balance the centrifugal force. These differences in pressure gradients in the plane perpendicular to the flow direction cause three-dimensional turbulent flows resulting in a higher pressure drop.

Bends and other flow obstructions also cause an increased fluid friction which generates an additional pressure drop. These frictional losses are a function of the wall roughness and the Reynold's number, but carry no weight in comparison to the other losses and are neglected in most cases.

The sum of the mentioned pressure losses along the fluid path between oil-water contact and well cause an increased hydrodynamic gradient and accordingly a lower critical production rate. Therefore, it is necessary to account for these pressure losses in highly complex flow geometries in naturally fractured reservoirs when predicted the maximum water free production rate.

Chapter 6

Conclusion

The scope of this study was to present an analytical solution for the maximum water-free production rate of horizontal wells in permeable faults. The presence of water coning in vertical faults in clastic and naturally fractured reservoirs was investigated and the numerical simulation verified by testing it against the analytical approach. Further, the influence of parameters like the fault thickness, permeability and the distance between the oil-water contact and the well were analyzed and boundary effects and turbulent flow behavior discussed.

For a fault model with specified porosity and permeability the analytical solution resulted in $2.59 \cdot 10^{-6}$ m^3/s and the numerical determination in $1.13 \cdot 10^{-5}$ m^3/s. This yields a relative error of 0.8 and shows that further studies could possibly improve the accuracy by considering the cone influence on the pressure distribution and boundary effects. To increase the accuracy of the simulations an implementation of the concept of relative permeabilities and capillary pressure effects is required. Therefore, I would recommended to use a commercial simulator which is commonly used in the oil and gas industry for faults with a lower permeability. However, the derived approximate solution is useful for a quick estimation of the critical rate. In case of increased flow velocities in highly permeable faults also inertial effects need to be considered where oil field simulators reach their limits.

The example of a flow through an open conduit representing a fault in a naturally fractured basement reservoir yielded an analytical value of $5.36 \cdot 10^{-4}$ m^3/s and a numerical critical rate of $8.48 \cdot 10^{-5}$ m^3/s. In this case a relative error of 3.3 was observed. This higher deviation is the result of the simplification of the analytical solution using the equation by Forchheimer. Significant inertial effects and turbulence were monitored and resultant discussions about the flow

through bends show their impact on the oil production in basement reservoir in countries like Vietnam, Indonesia, Venezuela and Brazil. Since this type of reservoir has attracted increased attention in the past years and are considered to have a large economic potential, a further improvement of the depletion methods should be of interest. Due to the mentioned rate-sensitive behavior of water coning, an accurate determination of the maximum water-free production rate is necessary to yield the desired economic and operational success in these regions.

Chapter 7

References

1. Ansari, R. Z., & Johns, R. T. (2006, January). Steady-state coning solutions with multiple wells and reservoir boundaries. In SPE/DOE Symposium on Improved Oil Recovery. Society of Petroleum Engineers.

2. ANSYS FLUENT 12.0 Theory Guide (April 2009)

3. Arthur, M. G. (1944). Fingering and coning of water and gas in homogeneous oil sand. Transactions of the AIME, 155(01), 184-201.

4. Batchelor, G. K. (1967). An introduction to fluid dynamics. Cambridge university press.

5. Beattie, D. R., & Roberts, B. E. (1996). Water Coning in Naturally Fractured Reservoirs. In SPE 35643 presented at the Gas Technology Conference held in Calgary, Alberta, Canada 28 April-1 May.

6. Bear, J. (2013). Dynamics of fluids in porous media. Courier Corporation.

7. Bernoulli, D. (1738). Specimen theoriae novae de mensura sortis. Commentarii Academiae Scientiarum Imperialis Petropolitanae, 5, 175–192.

8. Bournazel, C., & Jeanson, B. (1971, January). Fast water-coning evaluation method. In Fall Meeting of the Society of Petroleum Engineers of AIME. Society of Petroleum Engineers.

9. Brush, D. J., & Thomson, N. R. (2003). Fluid flow in synthetic rough‐walled fractures: Navier‐Stokes, Stokes, and local cubic law simulations. Water Resources Research, 39(4).

10. Chaney, P. E., Noble, M. D., Henson, W. L., & Rice, T. D. (1956). How to perforate your well to prevent water and gas coning. Oil Gas J, 55(53), 108-114.

11. Chaperon, I. (1986, January). Theoretical study of coning toward horizontal and vertical wells in anisotropic formations: subcritical and critical rates. In SPE Annual Technical Conference and Exhibition. Society of Petroleum Engineers.

12. Chappelear, J. E., & Hirasaki, G. J. (1976). A Model of Oil-Water Coning for Two-Dimensional Areal Reservoir Simulation. Society of Petroleum Engineers Journal, 16(02), 65-72.

13. Chierici, G. L., Ciucci, G. M., & Pizzi, G. (1964). A systematic study of gas and water coning by potentiometric models. Journal of Petroleum Technology, 16(08), 923-929.

14. Chisholm, D. (1980). Two-phase flow in bends. International Journal of Multiphase Flow, 6(4), 363-367.

15. Darcy, H. (1856). Les Fontaines Publiques de la Ville de Dijon. Dalmont, Paris.

16. Delhaye, J. M., & Riethmuller, M. L. (1981). Thermohydraulics of two-phase systems for industrial design and nuclear engineering. Hemisphere Pub. Corp.

17. Dupuit, A. J. E. J., & Dupuit, J. (1863). Études théoriques et pratiques sur la mouvement des eaux dans les canaux découverts et à travers les terrains perméables: avec des considérations relatives au régime des grandes eaux, au débouché à leur donner, et à la marche des alluvions dans les rivières à fond mobile. Dunod.

18. Forchheimer, P. (1901). Water movement through ground. Zeitschrift des Vereins Deutscher Ingenieure, 45, 1782-1788.

19. Fourar, M., & Bories, S. (1995). Experimental study of air-water two-phase flow through a fracture (narrow channel). International journal of multiphase flow, 21(4), 621-637.

20. Fourar, M., & Lenormand, R. (2000). Inertial effects in two-phase flow through fractures. Oil & Gas Science and Technology, 55(3), 259-268.

21. Fourar, M., Lenormand, R., Karimi-Fard, M., & Horne, R. (2005). Inertia effects in high-rate flow through heterogeneous porous media. Transport in Porous Media, 60(3), 353-370.

22. Gessner, F. B. (1973). The origin of secondary flow in turbulent flow along a corner. Journal of Fluid Mechanics, 58(01), 1-25.

23. Guo, B., Molinard, J. E., & Lee, R. L. (1992, January). A general solution of gas/water coning problem for horizontal wells. In European Petroleum Conference. Society of Petroleum Engineers.

24. Hele-Shaw, H. 1898. Flow of liquids in thin films. Nature 58: 34-36

25. Hirt, C. W., & Nichols, B. D. (1981). Volume of fluid (VOF) method for the dynamics of free boundaries. Journal of computational physics, 39(1), 201-225.

26. Høyland, L. A., Papatzacos, P., & Skjaeveland, S. M. (1989). Critical rate for water coning: correlation and analytical solution. SPE Reservoir Engineering, 4(04), 495-502.

27. Issa, R. I. (1986). Solution of the implicitly discretised fluid flow equations by operator-splitting. Journal of computational physics, 62(1), 40-65.

28. Johns, R. T., Lake, L. W., & Delliste, A. M. (2002, January 1). Prediction of Capillary Fluid Interfaces During Gas or Water Coning in Vertical Wells. Society of Petroleum Engineers.

29. Karcher, B. J., Giger, F. M., & Combe, J. (1986, January). Some practical formulas to predict horizontal well behavior. In SPE Annual Technical Conference and Exhibition. Society of Petroleum Engineers.

30. Kosakowski, G., & Berkowitz, B. (1999). Flow pattern variability in natural fracture intersections. Geophysical research letters, 26(12), 1765-1768.

31. Lockhart, R. W. and R. C. Martinelli, 1949.Proposed Correlation of Data for Isothermal Two-phase, Two-component Flow in Pipes, Chern. Eng. Prog., 45,39.

32. MacDonald, R. C. (1970). Methods for numerical simulation of water and gas coning. Society of Petroleum Engineers Journal, 10(04), 425-436.

33. Manzocchi, T., Walsh, J. J., Nell, P., & Yielding, G. (1999). Fault transmissibility multipliers for flow simulation models. Petroleum Geoscience, 5(1), 53-63.

34. Menouar, H. K., & Hakim, A. A. (1995). Water coning and critical rates in vertical and horizontal wells. In Middle East oil show & conference.

35. Muskat, M., & Wycokoff, R. D. (1935). An approximate theory of water-coning in oil production. Transactions of the AIME, 114(01), 144-163.

36. Nowamooz, A., Radilla, G., & Fourar, M. (2009). Non‐Darcian two‐phase flow in a transparent replica of a rough‐walled rock fracture. Water resources research, 45(7).

37. Prandtl, L. (1952). Essentials of fluid dynamics: With applications to hydraulics aeronautics, meteorology, and other subjects. Hafner Pub. Co..

38. Schols, R. S. (1972). An empirical formula for the critical oil production rate. Erdoel Erdgas, 88(1), 6-11.

39. Sobocinski, D. P., & Cornelius, A. (1965). A correlation for predicting water coning time. Journal of Petroleum Technology, 17(05), 594-600.

40. Sperrevik, S., Gillespie, P. A., Fisher, Q. J., Halvorsen, T., & Knipe, R. J. (2002). Empirical estimation of fault rock properties. Norwegian Petroleum Society Special Publications, 11, 109-125.

41. Van Golf-Racht, T. D. (1994, January). Water-coning in a fractured reservoir. In SPE Annual Technical Conference and Exhibition. Society of Petroleum Engineers.

42. Wheatley, M. J. (1985, January). An approximate theory of oil/water coning. In *SPE Annual Technical Conference and Exhibition*. Society of Petroleum Engineers.

43. Witherspoon, P. A., Wang, J. S. Y., Iwai, K., & Gale, J. E. (1980). Validity of cubic law for fluid flow in a deformable rock fracture. Water resources research, 16(6), 1016-1024.

44. Zimmerman, R. W., & Bodvarsson, G. S. (1996). Hydraulic conductivity of rock fractures. *Transport in porous media*, *23*(1), 1-30.

Appendix

8.1 Simulation input: Clastic environment

```
FLUENT
Version: 2d, pbns, vof, lam (2d, pressure-based, VOF, laminar)
Release: 14.0.0
Title:

Models
------

   Model                         Settings
   ------------------------------------
   Space                         2D
   Time                          Steady
   Viscous                       Laminar
   Heat Transfer                 Disabled
   Solidification and Melting    Disabled
   Species                       Disabled
   Coupled Dispersed Phase       Disabled
   NOx Pollutants                Disabled
   SOx Pollutants                Disabled
   Soot                          Disabled
   Mercury Pollutants            Disabled

Material Properties
-------------------

   Material: calcium-carbonate (solid)

      Property               Units    Method     Value(s)
      ------------------------------------------------
      Density                kg/m3    constant   2800
      Cp (Specific Heat)     j/kg-k   constant   856
      Thermal Conductivity   w/m-k    constant   2.25

   Material: water-liquid (fluid)

      Property                          Units      Method     Value(s)
      ------------------------------------------------------------------
      Density                           kg/m3      constant   1000
      Cp (Specific Heat)                j/kg-k     constant   4182
      Thermal Conductivity              w/m-k      constant   0.6
      Viscosity                         kg/m-s     constant   0.0049999
      Molecular Weight                  kg/kgmol   constant   18.0152
      Thermal Expansion Coefficient     1/k        constant   0
      Speed of Sound                    m/s        none       #f

   Material: oil (fluid)

      Property                          Units      Method     Value(s)
      ------------------------------------------------------------------
      Density                           kg/m3      constant   850
      Cp (Specific Heat)                j/kg-k     constant   1845
      Thermal Conductivity              w/m-k      constant   0.145
      Viscosity                         kg/m-s     constant   0.0049999
```

```
      Molecular Weight                kg/kgmol   constant   28
      Thermal Expansion Coefficient   1/k        constant   0
      Speed of Sound                  m/s        none       #f

Cell Zone Conditions
--------------------

   Zones

      name    id   type
      ------------------
      water   14   fluid
      oil     15   fluid

   Setup Conditions

      water

         Condition                                                  Value
         ------------------------------------------------------------
------------------------------------------------------------------------
-----------------------------------
         Material Name                                              engine-
oil
         Specify source terms?                                      no
         Source Terms                                               ((x-
momentum) (y-momentum))
         Specify fixed values?                                      no
         Fixed Values                                               ((x-
velocity (inactive . #f) (constant . 0) (profile  )) (y-velocity
(inactive . #f) (constant . 0) (profile  )))
         Frame Motion?                                              no
         Relative To Cell Zone                                      -1
         Reference Frame Rotation Speed (rad/s)                     0
         Reference Frame X-Velocity Of Zone (m/s)                   0
         Reference Frame Y-Velocity Of Zone (m/s)                   0
         Reference Frame X-Origin of Rotation-Axis (m)              0
         Reference Frame Y-Origin of Rotation-Axis (m)              0
         Reference Frame User Defined Zone Motion Function          none
         Mesh Motion?                                               no
         Relative To Cell Zone                                      -1
         Moving Mesh Rotation Speed (rad/s)                         0
         Moving Mesh X-Velocity Of Zone (m/s)                       0
         Moving Mesh Y-Velocity Of Zone (m/s)                       0
         Moving Mesh X-Origin of Rotation-Axis (m)                  0
         Moving Mesh Y-Origin of Rotation-Axis (m)                  0
         Moving Mesh User Defined Zone Motion Function              none
         Deactivated Thread                                         no
         Embedded Subgrid-Scale Model                               0
         Momentum Spatial Discretization                            0
         Cwale                                                      0.325
         Cs                                                         0.1
         Porous zone?                                               yes
         Porosity                                                   0.1
         Interfacial Area Density (1/m)                             1
         Heat Transfer Coefficient (w/m2-k)                         1

      oil
```

```
         Condition                                                Value
         ------------------------------------------------------------
------------------------------------------------------------------
-----------------------------------
         Material Name                                            engine-
oil
         Specify source terms?                                    no
         Source Terms                                             ((x-
momentum) (y-momentum))
         Specify fixed values?                                    no
         Fixed Values                                             ((x-
velocity (inactive . #f) (constant . 0) (profile  )) (y-velocity
(inactive . #f) (constant . 0) (profile  )))
         Frame Motion?                                            no
         Relative To Cell Zone                                    -1
         Reference Frame Rotation Speed (rad/s)                   0
         Reference Frame X-Velocity Of Zone (m/s)                 0
         Reference Frame Y-Velocity Of Zone (m/s)                 0
         Reference Frame X-Origin of Rotation-Axis (m)            0
         Reference Frame Y-Origin of Rotation-Axis (m)            0
         Reference Frame User Defined Zone Motion Function        none
         Mesh Motion?                                             no
         Relative To Cell Zone                                    -1
         Moving Mesh Rotation Speed (rad/s)                       0
         Moving Mesh X-Velocity Of Zone (m/s)                     0
         Moving Mesh Y-Velocity Of Zone (m/s)                     0
         Moving Mesh X-Origin of Rotation-Axis (m)                0
         Moving Mesh Y-Origin of Rotation-Axis (m)                0
         Moving Mesh User Defined Zone Motion Function            none
         Deactivated Thread                                       no
         Embedded Subgrid-Scale Model                             0
         Momentum Spatial Discretization                          0
         Cwale                                                    0.325
         Cs                                                       0.1
         Porous zone?                                             yes
         Porosity                                                 0.1
         Interfacial Area Density (1/m)                           1
         Heat Transfer Coefficient (w/m2-k)                       1

Boundary Conditions
-------------------

   Zones

      name          id   type
      --------------------------------
      owc-shadow    2    wall
      owc           19   wall
      well          18   velocity-inlet
      waterright    21   pressure-inlet
      waterleft     23   pressure-inlet
      oilright      22   pressure-inlet
      oilleft       24   pressure-inlet
      bottom        20   wall
      top           25   wall


   Setup Conditions

      owc-shadow
```

Condition	Value
Wall Motion	0
Shear Boundary Condition	0
Define wall motion relative to adjacent cell zone?	yes
Apply a rotational velocity to this wall?	no
Velocity Magnitude (m/s)	0
X-Component of Wall Translation	1
Y-Component of Wall Translation	0
Define wall velocity components?	no
X-Component of Wall Translation (m/s)	0
Y-Component of Wall Translation (m/s)	0
Rotation Speed (rad/s)	0
X-Position of Rotation-Axis Origin (m)	0
Y-Position of Rotation-Axis Origin (m)	0
X-component of shear stress (pascal)	0
Y-component of shear stress (pascal)	0
Fslip constant	0
Eslip constant	0
Specularity Coefficient	0

owc

Condition	Value
Wall Motion	0
Shear Boundary Condition	0
Define wall motion relative to adjacent cell zone?	yes
Apply a rotational velocity to this wall?	no
Velocity Magnitude (m/s)	0
X-Component of Wall Translation	1
Y-Component of Wall Translation	0
Define wall velocity components?	no
X-Component of Wall Translation (m/s)	0
Y-Component of Wall Translation (m/s)	0
Rotation Speed (rad/s)	0
X-Position of Rotation-Axis Origin (m)	0
Y-Position of Rotation-Axis Origin (m)	0
X-component of shear stress (pascal)	0
Y-component of shear stress (pascal)	0
Fslip constant	0
Eslip constant	0
Specularity Coefficient	0

well

Condition	Value
Velocity Specification Method	2
Reference Frame	0
Velocity Magnitude (m/s)	-0.0013
Supersonic/Initial Gauge Pressure (pascal)	0
X-Velocity (m/s)	0
Y-Velocity (m/s)	0
X-Component of Flow Direction	1
Y-Component of Flow Direction	0
X-Component of Axis Direction	1
Y-Component of Axis Direction	0
Z-Component of Axis Direction	0
X-Coordinate of Axis Origin (m)	0
Y-Coordinate of Axis Origin (m)	0

```
         Z-Coordinate of Axis Origin (m)              0
         Angular velocity (rad/s)                     0
         is zone used in mixing-plane model?          no

      waterright

         Condition                                    Value
         -------------------------------------------------------------
         Reference Frame                              0
         Gauge Total Pressure                         (profile
waterright water1)
         Supersonic/Initial Gauge Pressure (pascal)   0
         Direction Specification Method               1
         Coordinate System                            0
         X-Component of Flow Direction                1
         Y-Component of Flow Direction                0
         X-Component of Flow Direction                1
         Y-Component of Flow Direction                0
         X-Component of Axis Direction                0
         Y-Component of Axis Direction                0
         Z-Component of Axis Direction                1
         X-Coordinate of Axis Origin (m)              0
         Y-Coordinate of Axis Origin (m)              0
         Z-Coordinate of Axis Origin (m)              0
         is zone used in mixing-plane model?          no

      waterleft

         Condition                                    Value
         -------------------------------------------------------------
         Reference Frame                              0
         Gauge Total Pressure                         (profile
waterleft water1)
         Supersonic/Initial Gauge Pressure (pascal)   0
         Direction Specification Method               1
         Coordinate System                            0
         X-Component of Flow Direction                1
         Y-Component of Flow Direction                0
         X-Component of Flow Direction                1
         Y-Component of Flow Direction                0
         X-Component of Axis Direction                0
         Y-Component of Axis Direction                0
         Z-Component of Axis Direction                1
         X-Coordinate of Axis Origin (m)              0
         Y-Coordinate of Axis Origin (m)              0
         Z-Coordinate of Axis Origin (m)              0
         is zone used in mixing-plane model?          no

      oilright

         Condition                                    Value
         -------------------------------------------------------------
         Reference Frame                              0
         Gauge Total Pressure                         (profile
oilright oil)
         Supersonic/Initial Gauge Pressure (pascal)   0
         Direction Specification Method               1
         Coordinate System                            0
         X-Component of Flow Direction                1
         Y-Component of Flow Direction                0
         X-Component of Flow Direction                1
```

```
   Y-Component of Flow Direction                0
   X-Component of Axis Direction                0
   Y-Component of Axis Direction                0
   Z-Component of Axis Direction                1
   X-Coordinate of Axis Origin (m)              0
   Y-Coordinate of Axis Origin (m)              0
   Z-Coordinate of Axis Origin (m)              0
   is zone used in mixing-plane model?          no

oilleft

   Condition                                    Value
   ------------------------------------------------------------
   Reference Frame                              0
   Gauge Total Pressure                         (profile
oilleft oil)
   Supersonic/Initial Gauge Pressure (pascal)   0
   Direction Specification Method               1
   Coordinate System                            0
   X-Component of Flow Direction                1
   Y-Component of Flow Direction                0
   X-Component of Flow Direction                1
   Y-Component of Flow Direction                0
   X-Component of Axis Direction                0
   Y-Component of Axis Direction                0
   Z-Component of Axis Direction                1
   X-Coordinate of Axis Origin (m)              0
   Y-Coordinate of Axis Origin (m)              0
   Z-Coordinate of Axis Origin (m)              0
   is zone used in mixing-plane model?          no

bottom

   Condition                                          Value
   ------------------------------------------------------------
   Wall Motion                                        0
   Shear Boundary Condition                           1
   Define wall motion relative to adjacent cell zone? yes
   Apply a rotational velocity to this wall?          no
   Velocity Magnitude (m/s)                           0
   X-Component of Wall Translation                    1
   Y-Component of Wall Translation                    0
   Define wall velocity components?                   no
   X-Component of Wall Translation (m/s)              0
   Y-Component of Wall Translation (m/s)              0
   Rotation Speed (rad/s)                             0
   X-Position of Rotation-Axis Origin (m)             0
   Y-Position of Rotation-Axis Origin (m)             0
   X-component of shear stress (pascal)               0
   Y-component of shear stress (pascal)               0
   Fslip constant                                     0
   Eslip constant                                     0
   Specularity Coefficient                            0

top

   Condition                                          Value
   ------------------------------------------------------------
   Wall Motion                                        0
   Shear Boundary Condition                           1
   Define wall motion relative to adjacent cell zone? yes
```

Apply a rotational velocity to this wall?	no
Velocity Magnitude (m/s)	0
X-Component of Wall Translation	1
Y-Component of Wall Translation	0
Define wall velocity components?	no
X-Component of Wall Translation (m/s)	0
Y-Component of Wall Translation (m/s)	0
Rotation Speed (rad/s)	0
X-Position of Rotation-Axis Origin (m)	0
Y-Position of Rotation-Axis Origin (m)	0
X-component of shear stress (pascal)	0
Y-component of shear stress (pascal)	0
Fslip constant	0
Eslip constant	0
Specularity Coefficient	0

Solver Settings

Equations

Equation	Solved
Flow	yes
Volume Fraction	yes

Numerics

Numeric	Enabled
Absolute Velocity Formulation	yes

Relaxation

Variable	Relaxation Factor
Pressure	0.3
Density	1
Body Forces	1
Momentum	0.7
Volume Fraction	0.5

Linear Solver

Variable	Solver Type	Termination Criterion	Residual Reduction Tolerance
Pressure	V-Cycle	0.1	
X-Momentum	Flexible	0.1	0.7
Y-Momentum	Flexible	0.1	0.7
Volume Fraction	Flexible	0.1	0.7

Pressure-Velocity Coupling

Parameter	Value
Type	PISO
Skewness-Neighbour Coupling	yes
Skewness Correction	1
Neighbour Correction	1

Discretization Scheme

Variable	Scheme
Pressure	PRESTO!
Momentum	Second Order Upwind
Volume Fraction	Compressive

Solution Limits

Quantity	Limit
Minimum Absolute Pressure	1
Maximum Absolute Pressure	5e+10
Minimum Temperature	1
Maximum Temperature	5000

8.2 Simulation input: Fractured environment

```
FLUENT
Version: 2d, pbns, vof, lam (2d, pressure-based, VOF, laminar)
Release: 14.0.0
Title:

Models
------

   Model                         Settings
   ------------------------------------
   Space                         2D
   Time                          Steady
   Viscous                       Laminar
   Heat Transfer                 Disabled
   Solidification and Melting    Disabled
   Species                       Disabled
   Coupled Dispersed Phase       Disabled
   NOx Pollutants                Disabled
   SOx Pollutants                Disabled
   Soot                          Disabled
   Mercury Pollutants            Disabled

Material Properties
-------------------

   Material: calcium-carbonate (solid)

      Property               Units    Method     Value(s)
      ------------------------------------------------
      Density                kg/m3    constant   2800
      Cp (Specific Heat)     j/kg-k   constant   856
      Thermal Conductivity   w/m-k    constant   2.25

   Material: water-liquid (fluid)

      Property                         Units      Method     Value(s)
      ------------------------------------------------------------
      Density                          kg/m3      constant   1000
      Cp (Specific Heat)               j/kg-k     constant   4182
      Thermal Conductivity             w/m-k      constant   0.6
      Viscosity                        kg/m-s     constant   0.0049999
      Molecular Weight                 kg/kgmol   constant   18.0152
      Thermal Expansion Coefficient    1/k        constant   0
      Speed of Sound                   m/s        none       #f

   Material: oil (fluid)

      Property                         Units      Method     Value(s)
      ------------------------------------------------------------
      Density                          kg/m3      constant   850
      Cp (Specific Heat)               j/kg-k     constant   1845
      Thermal Conductivity             w/m-k      constant   0.145
      Viscosity                        kg/m-s     constant   0.0049999
      Molecular Weight                 kg/kgmol   constant   28
      Thermal Expansion Coefficient    1/k        constant   0
      Speed of Sound                   m/s        none       #f
```

```
Cell Zone Conditions
--------------------

   Zones

      name    id   type
      ------------------
      oil     15   fluid
      water   14   fluid

   Setup Conditions

      oil

         Condition                                                  Value
         ------------------------------------------------------------
------------------------------------------------------------------------
-----------------------------------
         Material Name                                              water-
liquid
         Specify source terms?                                      no
         Source Terms                                               ((x-
momentum) (y-momentum))
         Specify fixed values?                                      no
         Fixed Values                                               ((x-
velocity (inactive . #f) (constant . 0) (profile  )) (y-velocity
(inactive . #f) (constant . 0) (profile  )))
         Frame Motion?                                              no
         Relative To Cell Zone                                      -1
         Reference Frame Rotation Speed (rad/s)                     0
         Reference Frame X-Velocity Of Zone (m/s)                   0
         Reference Frame Y-Velocity Of Zone (m/s)                   0
         Reference Frame X-Origin of Rotation-Axis (m)              0
         Reference Frame Y-Origin of Rotation-Axis (m)              0
         Reference Frame User Defined Zone Motion Function          none
         Mesh Motion?                                               no
         Relative To Cell Zone                                      -1
         Moving Mesh Rotation Speed (rad/s)                         0
         Moving Mesh X-Velocity Of Zone (m/s)                       0
         Moving Mesh Y-Velocity Of Zone (m/s)                       0
         Moving Mesh X-Origin of Rotation-Axis (m)                  0
         Moving Mesh Y-Origin of Rotation-Axis (m)                  0
         Moving Mesh User Defined Zone Motion Function              none
         Deactivated Thread                                         no
         Embedded Subgrid-Scale Model                               0
         Momentum Spatial Discretization                            0
         Cwale                                                      0.325
         Cs                                                         0.1
         Porous zone?                                               yes
         Porosity                                                   1
         Interfacial Area Density (1/m)                             1
         Heat Transfer Coefficient (w/m2-k)                         1

      water
```

```
         Condition                                                Value
         ---------------------------------------------------------
-------------------------------------------------------------------
-----------------------------------
         Material Name                                            water-
liquid
         Specify source terms?                                    no
         Source Terms                                             ((x-
momentum) (y-momentum))
         Specify fixed values?                                    no
         Fixed Values                                             ((x-
velocity (inactive . #f) (constant . 0) (profile  )) (y-velocity
(inactive . #f) (constant . 0) (profile  )))
         Frame Motion?                                            no
         Relative To Cell Zone                                    -1
         Reference Frame Rotation Speed (rad/s)                   0
         Reference Frame X-Velocity Of Zone (m/s)                 0
         Reference Frame Y-Velocity Of Zone (m/s)                 0
         Reference Frame X-Origin of Rotation-Axis (m)            0
         Reference Frame Y-Origin of Rotation-Axis (m)            0
         Reference Frame User Defined Zone Motion Function        none
         Mesh Motion?                                             no
         Relative To Cell Zone                                    -1
         Moving Mesh Rotation Speed (rad/s)                       0
         Moving Mesh X-Velocity Of Zone (m/s)                     0
         Moving Mesh Y-Velocity Of Zone (m/s)                     0
         Moving Mesh X-Origin of Rotation-Axis (m)                0
         Moving Mesh Y-Origin of Rotation-Axis (m)                0
         Moving Mesh User Defined Zone Motion Function            none
         Deactivated Thread                                       no
         Embedded Subgrid-Scale Model                             0
         Momentum Spatial Discretization                          0
         Cwale                                                    0.325
         Cs                                                       0.1
         Porous zone?                                             yes
         Porosity                                                 1
         Interfacial Area Density (1/m)                           1
         Heat Transfer Coefficient (w/m2-k)                       1

Boundary Conditions
-------------------

   Zones

      name          id   type
      ---------------------------------
      well          18   velocity-inlet
      waterright    21   pressure-inlet
      waterleft     23   pressure-inlet
      oilright      22   pressure-inlet
      oilleft       24   pressure-inlet
      bottom        20   wall
      top           25   wall

   Setup Conditions

      well

         Condition                                    Value
         -------------------------------------------------
         Velocity Specification Method                2
```

```
         Reference Frame                              0
         Velocity Magnitude (m/s)                     -0.009
         Supersonic/Initial Gauge Pressure (pascal)   0
         X-Velocity (m/s)                             0
         Y-Velocity (m/s)                             0
         X-Component of Flow Direction                1
         Y-Component of Flow Direction                0
         X-Component of Axis Direction                1
         Y-Component of Axis Direction                0
         Z-Component of Axis Direction                0
         X-Coordinate of Axis Origin (m)              0
         Y-Coordinate of Axis Origin (m)              0
         Z-Coordinate of Axis Origin (m)              0
         Angular velocity (rad/s)                     0
         is zone used in mixing-plane model?          no

      waterright

         Condition                                    Value
         ------------------------------------------------------------
------------
         Reference Frame                              0
         Gauge Total Pressure                         (profile
waterright water1)
         Supersonic/Initial Gauge Pressure (pascal)   0
         Direction Specification Method               1
         Coordinate System                            0
         X-Component of Flow Direction                1
         Y-Component of Flow Direction                0
         X-Component of Flow Direction                1
         Y-Component of Flow Direction                0
         X-Component of Axis Direction                0
         Y-Component of Axis Direction                0
         Z-Component of Axis Direction                1
         X-Coordinate of Axis Origin (m)              0
         Y-Coordinate of Axis Origin (m)              0
         Z-Coordinate of Axis Origin (m)              0
         is zone used in mixing-plane model?          no

      waterleft

         Condition                                    Value
         ------------------------------------------------------------
-----------
         Reference Frame                              0
         Gauge Total Pressure                         (profile
waterleft water1)
         Supersonic/Initial Gauge Pressure (pascal)   0
         Direction Specification Method               1
         Coordinate System                            0
         X-Component of Flow Direction                1
         Y-Component of Flow Direction                0
         X-Component of Flow Direction                1
         Y-Component of Flow Direction                0
         X-Component of Axis Direction                0
         Y-Component of Axis Direction                0
         Z-Component of Axis Direction                1
         X-Coordinate of Axis Origin (m)              0
         Y-Coordinate of Axis Origin (m)              0
         Z-Coordinate of Axis Origin (m)              0
         is zone used in mixing-plane model?          no
```

```
      oilright

         Condition                                        Value
         ------------------------------------------------------------
-------
         Reference Frame                                  0
         Gauge Total Pressure                             (profile
oilright oil)
         Supersonic/Initial Gauge Pressure (pascal)       0
         Direction Specification Method                   1
         Coordinate System                                0
         X-Component of Flow Direction                    1
         Y-Component of Flow Direction                    0
         X-Component of Flow Direction                    1
         Y-Component of Flow Direction                    0
         X-Component of Axis Direction                    0
         Y-Component of Axis Direction                    0
         Z-Component of Axis Direction                    1
         X-Coordinate of Axis Origin (m)                  0
         Y-Coordinate of Axis Origin (m)                  0
         Z-Coordinate of Axis Origin (m)                  0
         is zone used in mixing-plane model?              no

      oilleft

         Condition                                        Value
         ------------------------------------------------------------
------
         Reference Frame                                  0
         Gauge Total Pressure                             (profile
oilleft oil)
         Supersonic/Initial Gauge Pressure (pascal)       0
         Direction Specification Method                   1
         Coordinate System                                0
         X-Component of Flow Direction                    1
         Y-Component of Flow Direction                    0
         X-Component of Flow Direction                    1
         Y-Component of Flow Direction                    0
         X-Component of Axis Direction                    0
         Y-Component of Axis Direction                    0
         Z-Component of Axis Direction                    1
         X-Coordinate of Axis Origin (m)                  0
         Y-Coordinate of Axis Origin (m)                  0
         Z-Coordinate of Axis Origin (m)                  0
         is zone used in mixing-plane model?              no

      bottom

         Condition                                              Value
         ------------------------------------------------------------
         Wall Motion                                            0
         Shear Boundary Condition                               1
         Define wall motion relative to adjacent cell zone?     yes
         Apply a rotational velocity to this wall?              no
         Velocity Magnitude (m/s)                               0
         X-Component of Wall Translation                        1
         Y-Component of Wall Translation                        0
         Define wall velocity components?                       no
         X-Component of Wall Translation (m/s)                  0
         Y-Component of Wall Translation (m/s)                  0
```

Rotation Speed (rad/s)	0
X-Position of Rotation-Axis Origin (m)	0
Y-Position of Rotation-Axis Origin (m)	0
X-component of shear stress (pascal)	0
Y-component of shear stress (pascal)	0
Fslip constant	0
Eslip constant	0
Specularity Coefficient	0

top

Condition	Value
Wall Motion	0
Shear Boundary Condition	1
Define wall motion relative to adjacent cell zone?	yes
Apply a rotational velocity to this wall?	no
Velocity Magnitude (m/s)	0
X-Component of Wall Translation	1
Y-Component of Wall Translation	0
Define wall velocity components?	no
X-Component of Wall Translation (m/s)	0
Y-Component of Wall Translation (m/s)	0
Rotation Speed (rad/s)	0
X-Position of Rotation-Axis Origin (m)	0
Y-Position of Rotation-Axis Origin (m)	0
X-component of shear stress (pascal)	0
Y-component of shear stress (pascal)	0
Fslip constant	0
Eslip constant	0
Specularity Coefficient	0

Solver Settings

Equations

Equation	Solved
Flow	yes
Volume Fraction	yes

Numerics

Numeric	Enabled
Absolute Velocity Formulation	yes

Relaxation

Variable	Relaxation Factor
Pressure	0.3
Density	1
Body Forces	1
Momentum	0.7
Volume Fraction	0.5

Linear Solver

	Solver	Termination	Residual Reduction

Variable	Type	Criterion	Tolerance
Pressure	V-Cycle	0.1	
X-Momentum	Flexible	0.1	0.7
Y-Momentum	Flexible	0.1	0.7
Volume Fraction	Flexible	0.1	0.7

Pressure-Velocity Coupling

Parameter	Value
Type	PISO
Skewness-Neighbour Coupling	yes
Skewness Correction	1
Neighbour Correction	1

Discretization Scheme

Variable	Scheme
Pressure	PRESTO!
Momentum	Second Order Upwind
Volume Fraction	Compressive

Solution Limits

Quantity	Limit
Minimum Absolute Pressure	1
Maximum Absolute Pressure	5e+10
Minimum Temperature	1
Maximum Temperature	5000